Quantum transport in graphene

L1 Disordered graphene (G)

L2 Ballistic electrons in graphene (G/hBN)

L3 Moiré superlattice effects in G/hBN heterostructures

tunnelling between almost aligned graphene flakes

moiré superlattice in van der Waals heterostructures

moiré minibands in G/hBN

Brown-Zak magnetic minibands in G/hBN

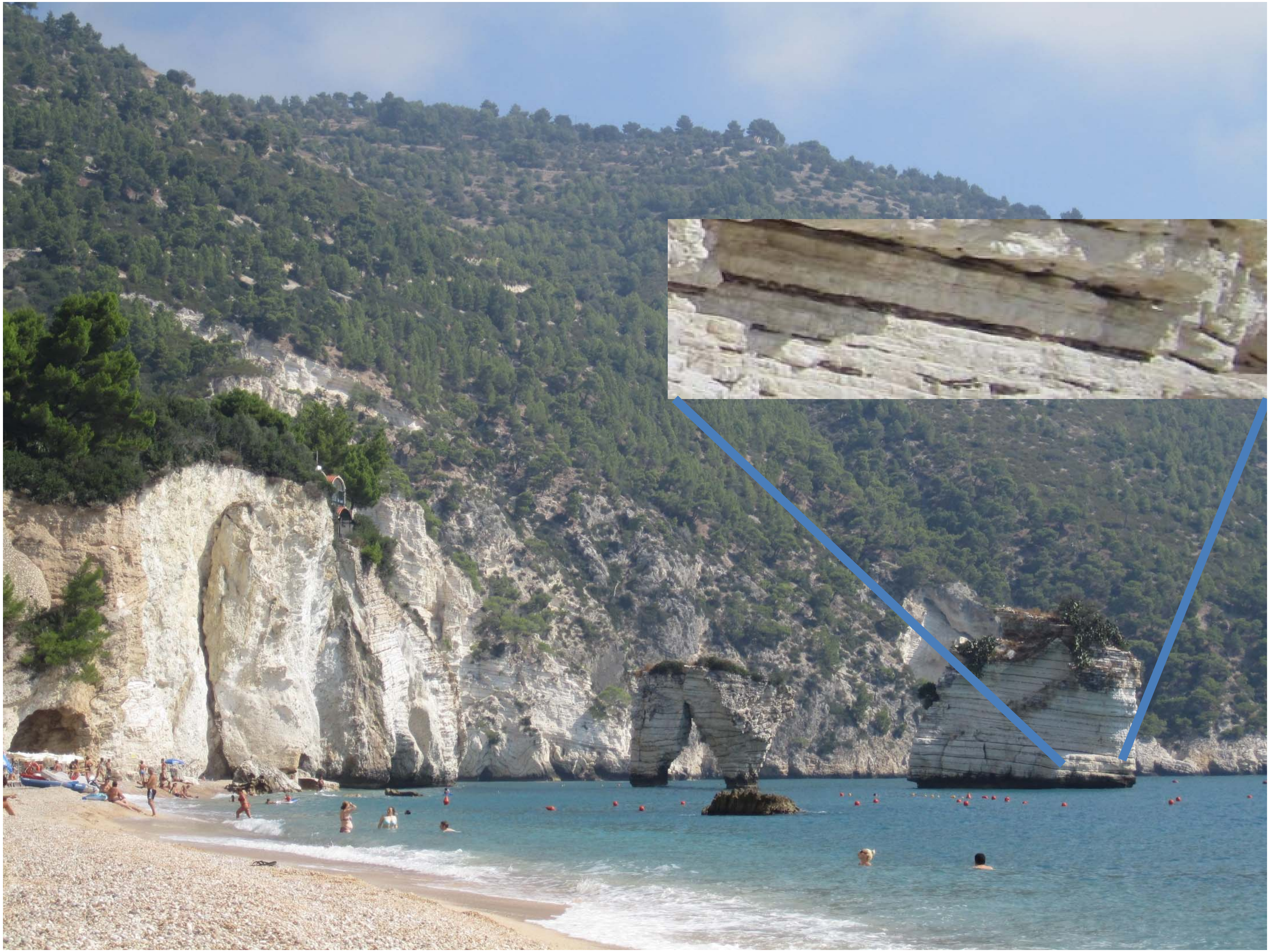

Momentum-conserving resonant tunnelling between graphene flakes in G/hBN/G structures

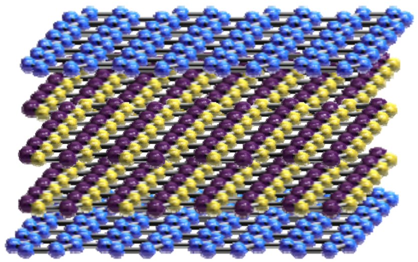

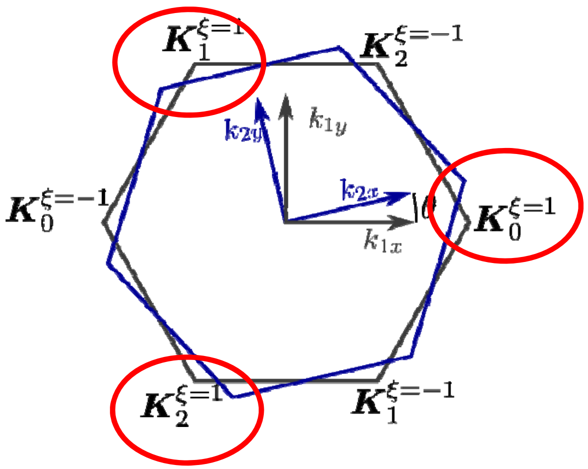

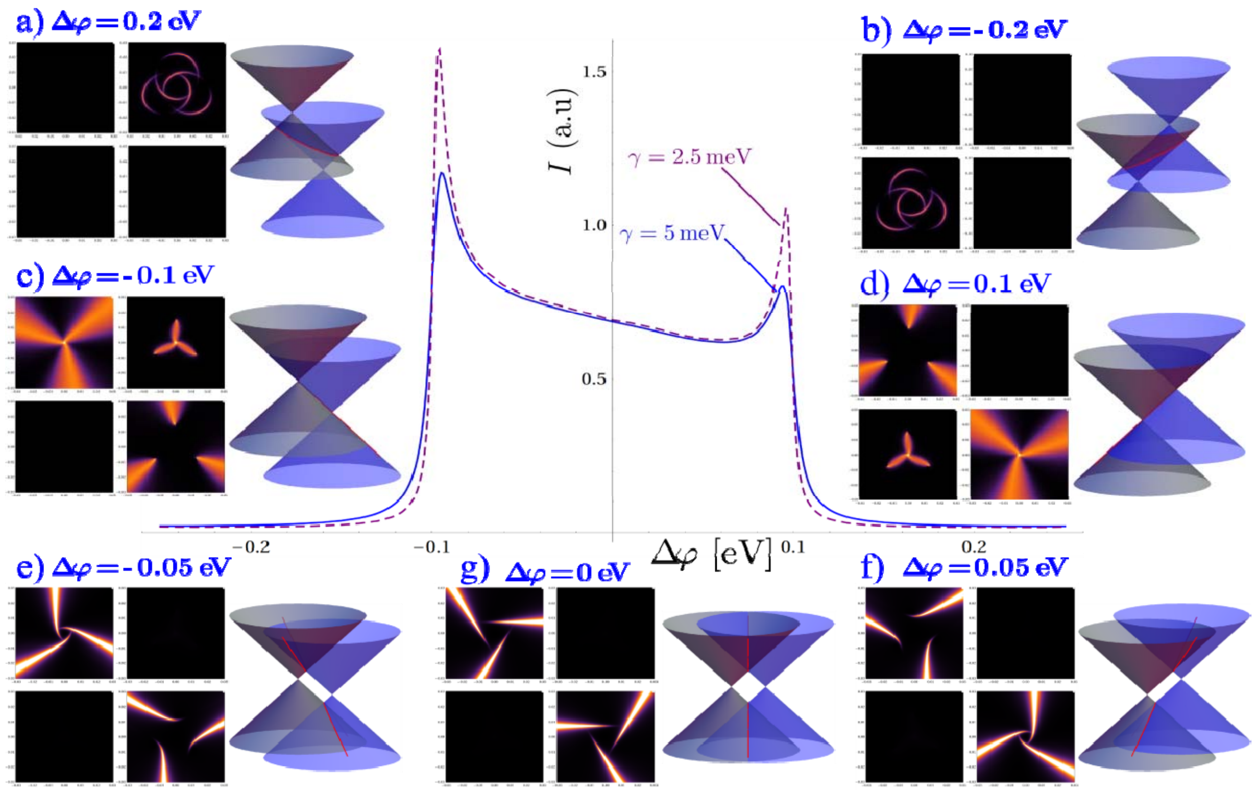

Mishchenko, Tu, Cao, Gorbachev, Wallbank, Greenaway, Morozov, Zhu, Wong, Withers, Woods, Kim, Watanabe, Taniguchi, Vdovin, Makarovsky, Fromhold, Fal'ko, Geim, Eaves, Novoselov - Nature Nanotechnology 9, 808 (2014)

Resonant tunnelling in almost aligned ballistic G/hBN/G structures

Exp (dI/dV_b)

Th (dI/dV_b)

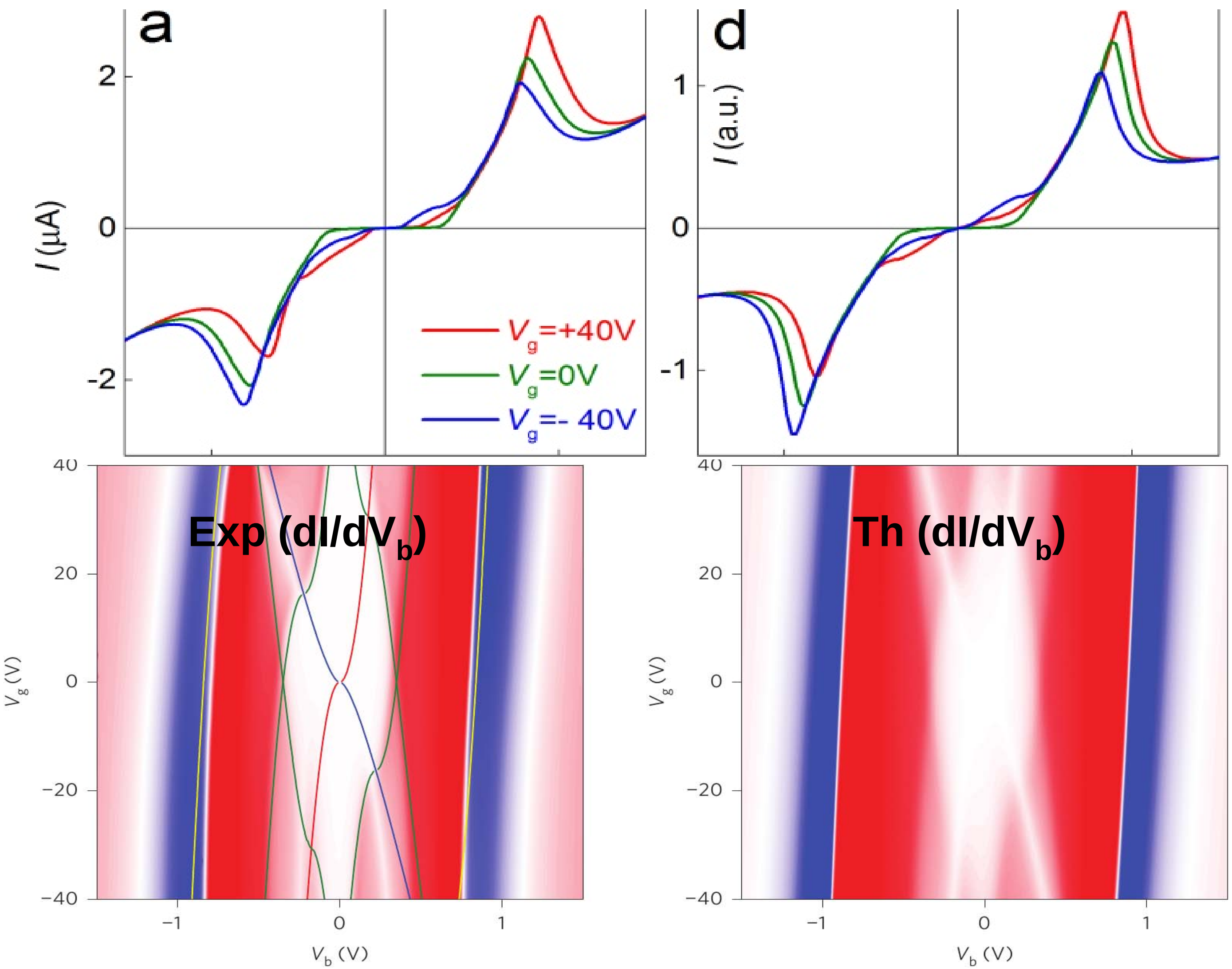

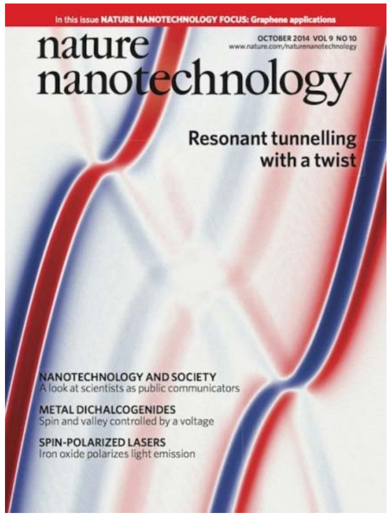

Mishchenko, Tu, Cao, Gorbachev, Wallbank, Greenaway, Morozov, Morozov, Zhu, Wong, Withers, Woods, Kim, Watanabe, Taniguchi, Vdovin, Makarovsky, Fromhold, Fal'ko, Geim, Eaves, Novoselov - Nature Nanotechnology 9, 808 (2014)

Momentum-conserving resonant tunnelling between almost aligned graphene flakes in G/hBN/G structures

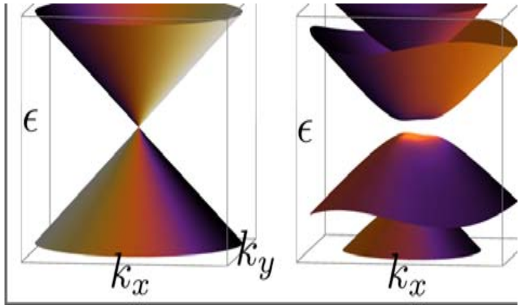

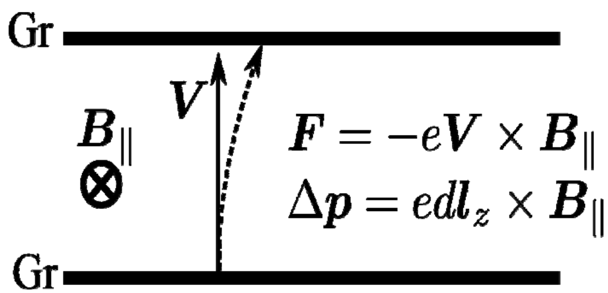

Gr-hBN-Gr

BLGr-hBN-Gr

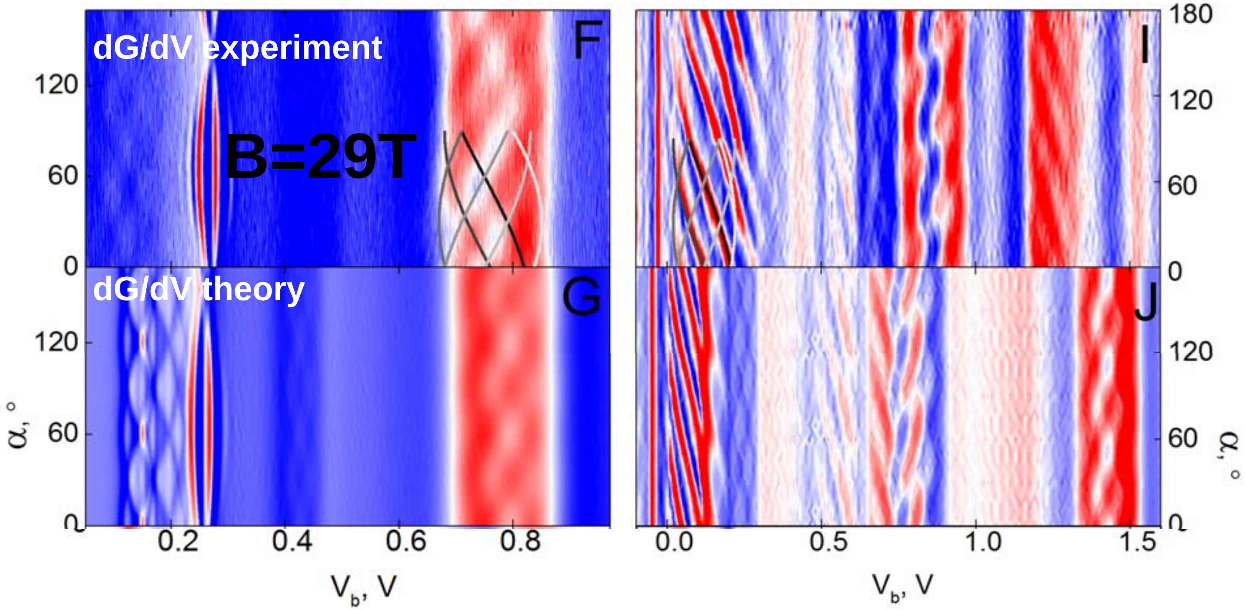

Lorentz boost: in-plane magnetic field distinguishes resonance tunneling conditions in six Brillouin zone corners, probed by rotating the in-plane magnetic field.

$$\Delta K_j \approx \theta l_z \times K_j + \Delta p$$

Wallbank, Ghazaryan, Misra, Cao, Tu, Piot, Potemski, Pezzini, Wiedmann, Zeitler, Lane, Morozov, Greenaway, Eaves, Geim, Fal'ko, Novoselov, Mishchenko - Science 353, 575 (2016)

Quantum transport in graphene

L1 Disordered graphene (G)

L2 Ballistic electrons in graphene (G/hBN)

L3 Moiré superlattice effects in G/hBN heterostructures

tunnelling between almost aligned graphene flakes

moiré superlattice in van der Waals heterostructures

moiré minibands in G/hBN

Brown-Zak magnetic minibands in G/hBN

Graphene: gapless semiconductor with Dirac electrons

$$\hat{H} = v\vec{\sigma}\cdot\vec{p}$$

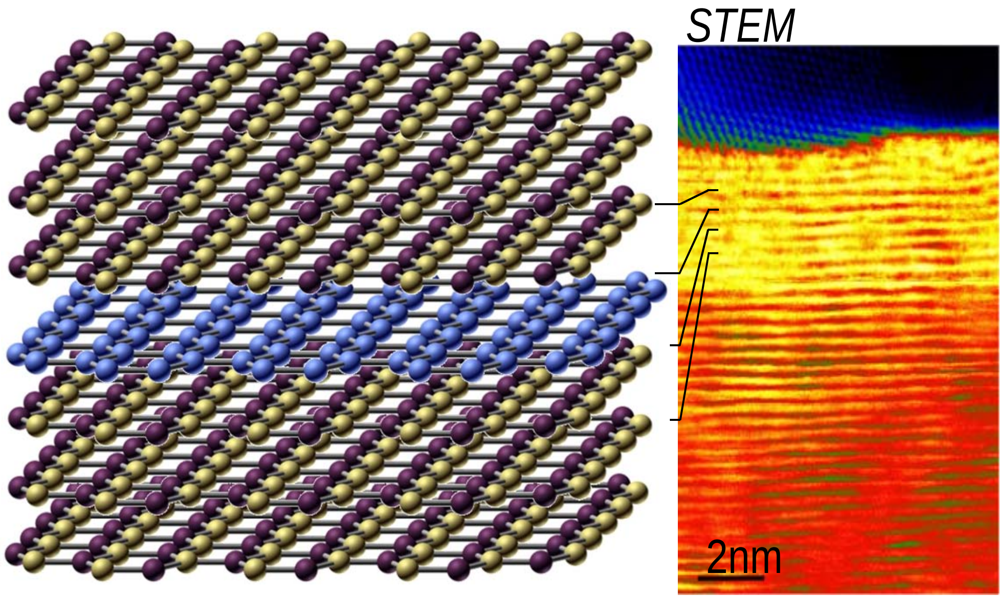

hBN ('white graphene') sp^2 – bonded insulator with a large band gap, Δ >5eV

$$\hat{H} = \Delta\sigma_z + v'\vec{\sigma}\cdot\vec{p}$$

- **Hexagonal boron nitride (hBN) is an ideal atomically flat substrate and insulating environment for graphene**
- **Almost aligned graphene – hBN heterostructures feature moiré superlattices generating moiré minibands for Dirac electrons in graphene and Zak-Brown magnetic minibands ('Hofstadter butterfly'), observable at high temperatures**

Moiré pattern

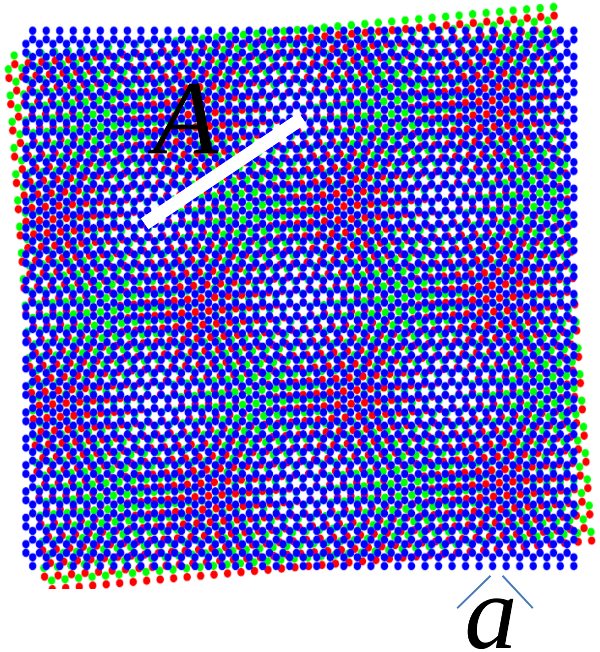

$$A \approx \frac{a}{\sqrt{\delta^2 + \theta^2}}$$

δ ↑ lattice mismatch 1.8% for G/hBN

θ ↑ misalignment

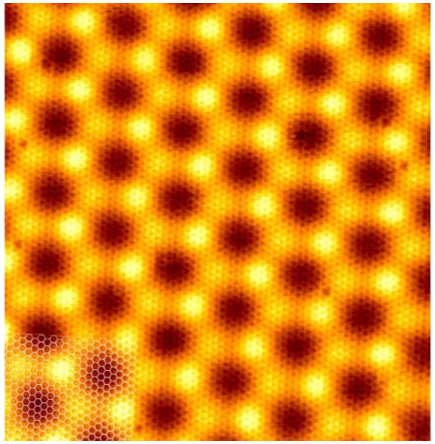

STM of graphene on Ir(111)
Busse et al
PRL 107, 036101 (2011)

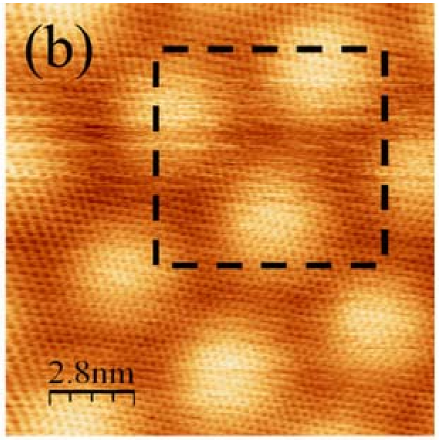

STM of graphene on Ni
Arramel et al
Graphene 2, 102 (2013)

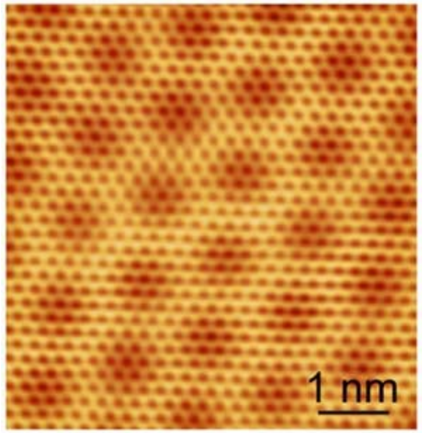

STM of G/hBN
Xue at al
Nature Mat. 10, 282–285 (2011)

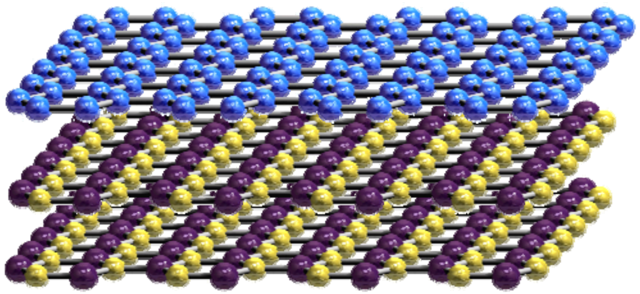

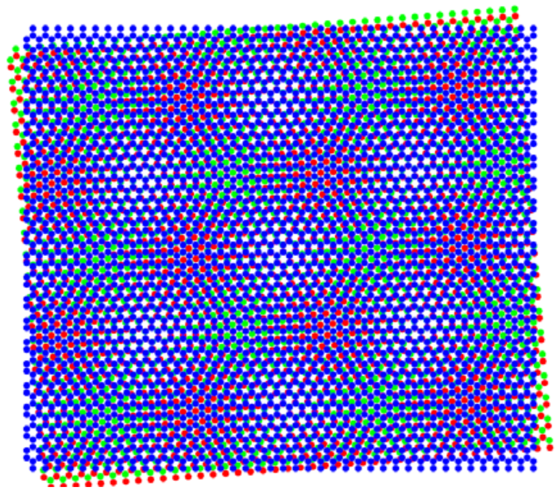

highly oriented graphene-BN:

$$A \sim 15\ nm$$

heterostructure with new electronic properties

Highly oriented graphene-hBN heterostructures (misalignment $\theta<1^o$) have been produced by groups of Geim & Novoselov (Manchester)

Ponomarenko, Gorbachev, Elias, Yu, Patel, Mayorov, Woods, Wallbank, Mucha-Kruczynski, Piot, Potemski, Grigorieva, Guinea, Novoselov, VF, Geim - Nature 497, 594 (2013)

Jarillo-Herrero & Ashoori (MIT), Kim & Hone (Columbia)

B Hunt, et al - Science 340, 1427 (2013)

CR Dean, et al, Nature 497, 598 (2013)

Graphene grown on hBN

CVD: Usachov *et al.*, PRB 82, 075415 (2010); Roth *et al.*, Nano Letters 13, 2668 (2013); Yang et al., Nature Mater. 12, 792 (2013), ….

400x400nm

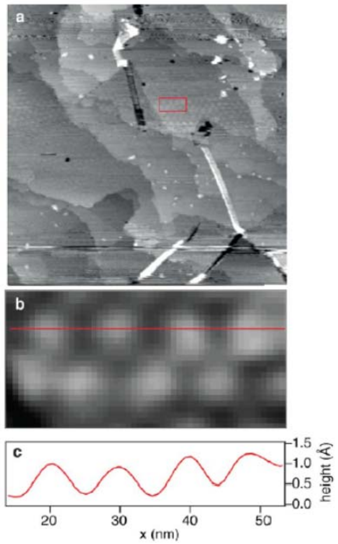

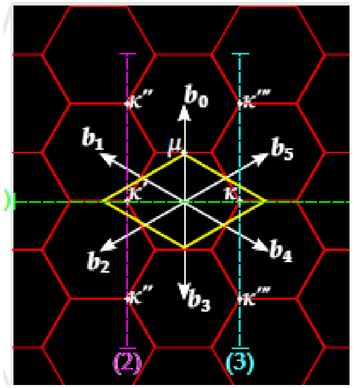

superlattice with period *A>>a* and reciprocal lattice (Bragg) vectors

$$\vec{b}_n = \vec{G}_n^{G} - \vec{G}_n^{hBN}$$

MBE: Summerfield, Davies, Cheng, Korolkov, Cho, Mellor, Foxon, Khlobystov, Watanabe, Taniguchi, Eaves, Novikov, Beton - Scientific Reports 6, 22440 (2016)

Quantum transport in graphene

L1 Disordered graphene (G)

L2 Ballistic electrons in graphene (G/hBN)

L3 Moiré superlattice effects in G/hBN heterostructures

tunnelling between almost aligned graphene flakes

moiré superlattice in van der Waals heterostructures

moiré minibands in G/hBN

Brown-Zak magnetic minibands in G/hBN

Separation between layers is larger than the lattice constant, hence, moiré perturbation is dominated by harmonics determined by simplest combinations of Bragg vectors of graphene and hBN (effect of higher harmonics is exponentially small)

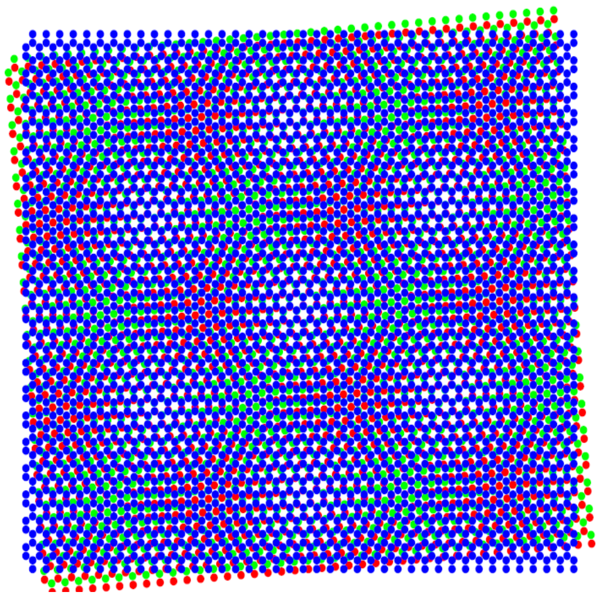

Lopes dos Santos, Peres, Castro Neto - PRL 99, 256802 (2007)
Lopes dos Santos, Peres, Castro Neto - arXiv:1202.1088 (2012)
Bistritzer, MacDonald - PRB 81, 245412 (2010)
Kindermann, Uchoa, Miller - Phys. Rev. B 86, 115415 (2012)

$$\vec{b}_0 = \vec{G}_G - \vec{G}_{BN} = \left[1 - (1+\delta)^{-1}\hat{R}_\theta\right]\begin{pmatrix}\frac{4\pi}{3a}\\ 0\end{pmatrix}$$

$$|\vec{b}_0| \equiv b \approx \frac{3\pi}{4a}\sqrt{\delta^2+\theta^2}$$

lattice mismatch 1.8% for G/hBN

misalignment $<5^0$

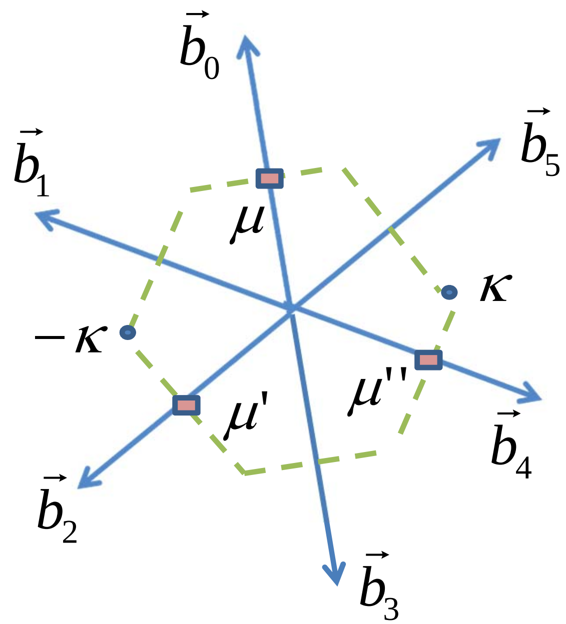

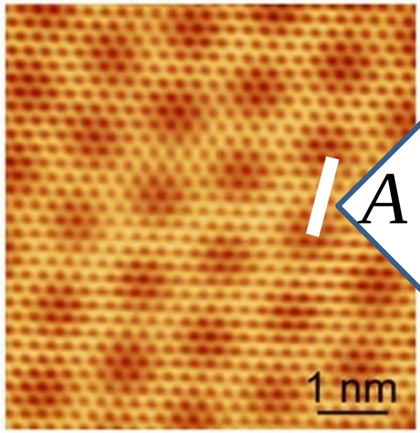

$$A \approx \frac{a}{\sqrt{\delta^2 + \theta^2}}$$

Xue, Sanchez-Yamagishi, Bulmash, Jacquod, Deshpande, Watanabe, Taniguchi, Jarillo-Herrero, LeRoy - Nature Mat 10, 282 (2011)

small misalignment

lattice mismatch

$\delta=0.018$ for non-strained graphene on hBN

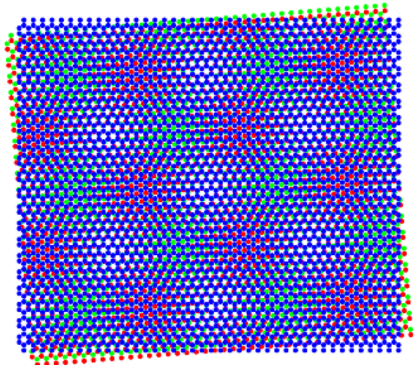

Long-period moiré patterns are generic for all G/hBN heterostructures, grown and mechanically transferred

Both graphene and hBN lattices are honeycomb,

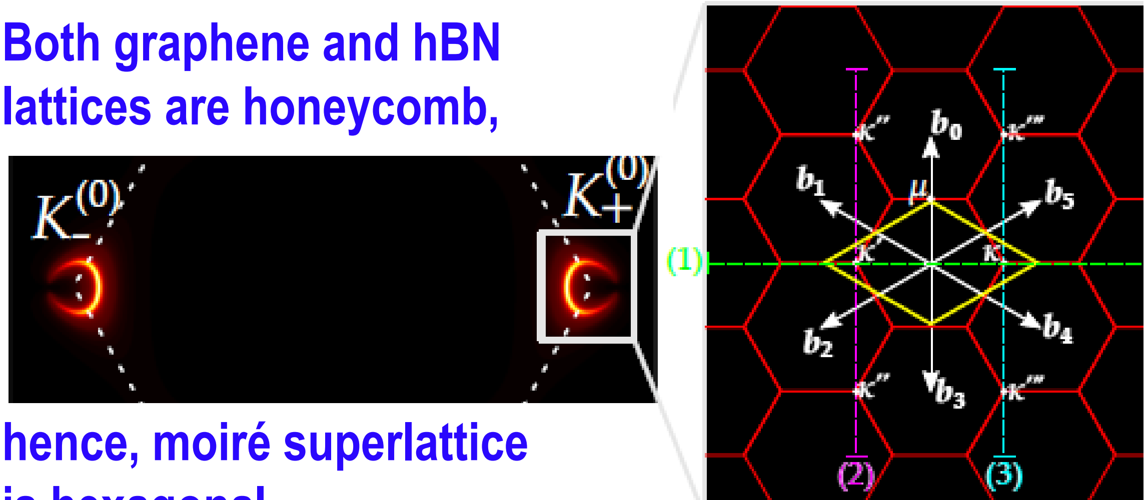

hence, moiré superlattice is hexagonal

$$\vec{b} = \vec{G}^G - \vec{G}^{hBN} = \frac{2\pi}{4A}$$

$$b_n \approx \frac{3\pi}{4a}\sqrt{\delta^2 + \theta^2} << K, G^G$$

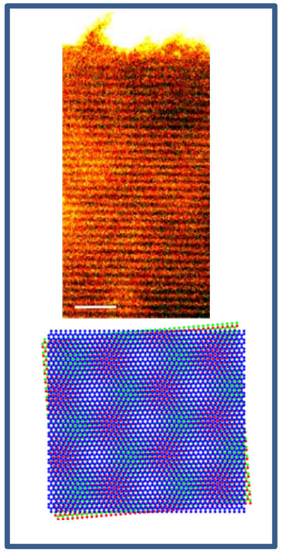

electrons in G/hBN moiré superlattices

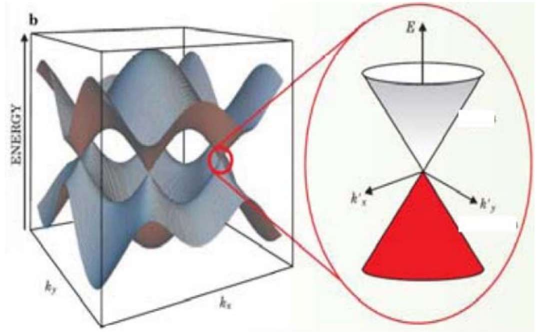

+

$$a_z > a \;\Rightarrow\; only\;\; \vec{b} = \vec{G}^{G} - \vec{G}^{hBN} \longrightarrow \delta H_{moire}$$

electrostatic modulation

sublattice asymmetry

hopping between sublattices, leading to a pseudomagnetic field

$$\hat{H} = v\boldsymbol{p}\cdot\boldsymbol{\sigma} + u_0 v b f_1(\boldsymbol{r}) + u_3 v b f_2(\boldsymbol{r})\sigma_3\tau_3 + u_1 v\left[\boldsymbol{l}_z \times \nabla f_2(\boldsymbol{r})\right]\cdot\boldsymbol{\sigma}\tau_3$$

inversion symmetric

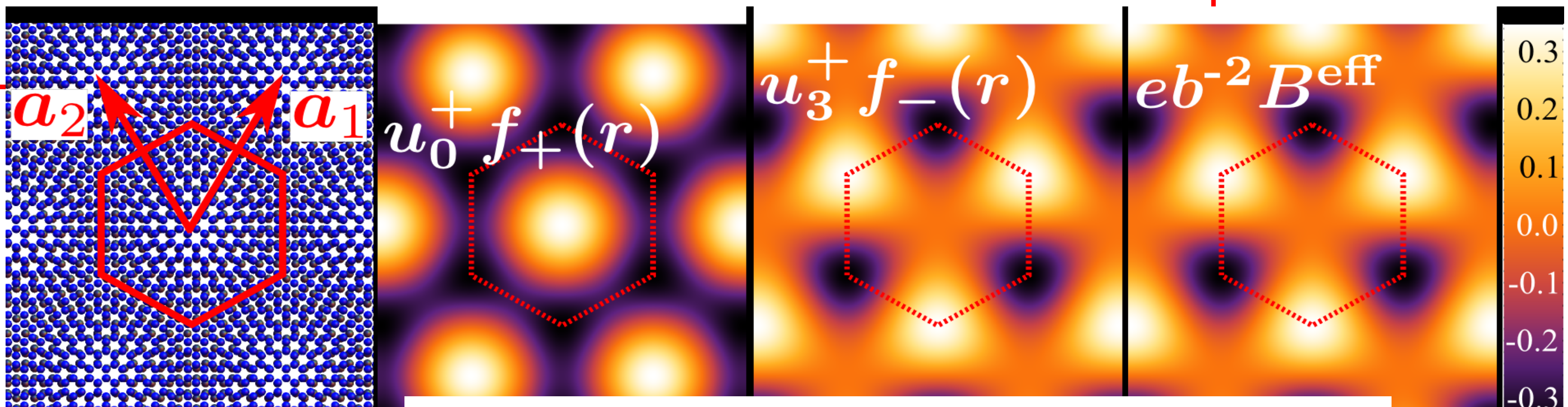

Wallbank, Patel, Mucha-Kruczynski, Geim, Fal'ko - PRB 87, 245408 (2013)

characteristic moiré miniband regimes: no electron-hole symmetry

three mini-DPs at the edge of 1st miniband

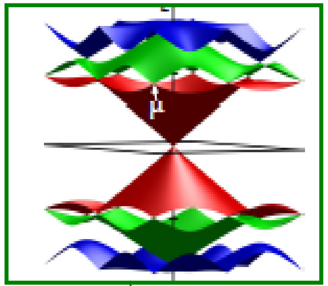

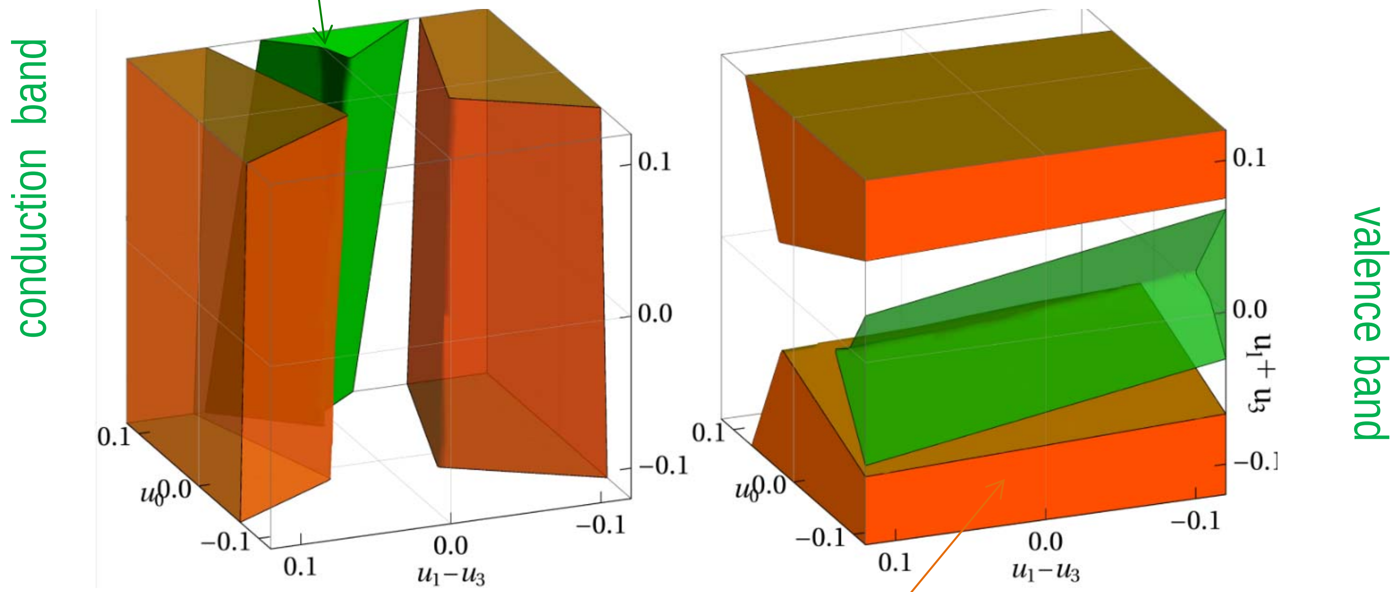

single mini-Dirac point at the edge of 1st miniband

vb

$v_{mDP} \approx \frac{1}{2} v$

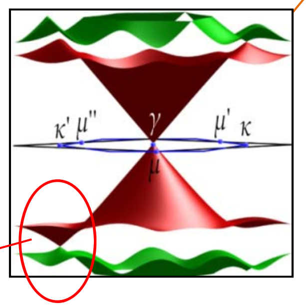

G-hBN hopping model and electric quadrupole moments on, e.g., nitrogen sites

vbu_0	vbu_1	vbu_3
$\frac{1}{2}u$	$-\frac{\delta}{\sqrt{\delta^2+\theta^2}}u$	$-\frac{\sqrt{3}}{2}u$

Wallbank, Patel, Mucha-Kruczynski, Geim, Fal'ko - PRB 87, 245408 (2013)

graphene sublattice — graphene valley

$$\hat{H} = v\boldsymbol{p}\cdot\boldsymbol{\sigma} + u_0 v b f_1(\boldsymbol{r}) + u_3 v b f_2(\boldsymbol{r})\sigma_3\tau_3 + u_1 v\left[\boldsymbol{l}_z \times \nabla f_2(\boldsymbol{r})\right]\cdot\boldsymbol{\sigma}\tau_3$$
$$+ \underline{\tilde{u}_0 v b f_2(\boldsymbol{r}) + \tilde{u}_3 v b f_1(\boldsymbol{r})\sigma_3\tau_3} + \tilde{u}_1 v\left[\boldsymbol{l}_z \times \nabla f_1(\boldsymbol{r})\right]\cdot\boldsymbol{\sigma}\tau_3$$

graphene lattice may adjust to the periodic modulation of vdW force

$$\vec{\ell}(\vec{r}) = \sum_m \vec{\ell}_m e^{i\vec{b}_m\vec{r}} \qquad u_i = u_i(d+\ell_z)$$

⇓

$$f_1(\boldsymbol{r}) = \sum_{m=0\ldots5} e^{i\boldsymbol{b}_m\cdot\boldsymbol{r}}\, e^{i\vec{G}_m\vec{\ell}(\vec{r})}$$
$$f_2(\boldsymbol{r}) = i\sum_{m=0\ldots5}(-1)^m e^{i\boldsymbol{b}_m\cdot\boldsymbol{r}}\, e^{i\vec{G}_m\vec{\ell}(\vec{r})}$$

⇓

San-Jose, Gutierrez, Sturla, Guinea - PRB 90, 075428 (2014)
Cosma, Wallbank, Cheainov, Fal'ko - Faraday Discussion 173 (2014)

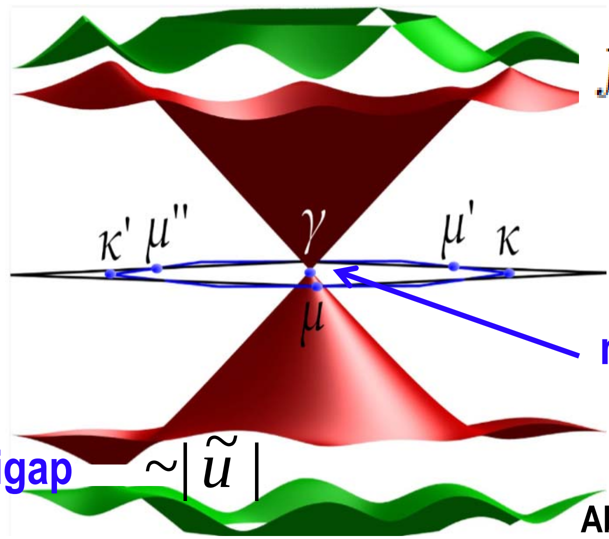

minigap at the band edge $\sim|\tilde{u}u| + |\vec{\ell}||\tilde{u}|$

minigap $\sim|\tilde{u}|$

Kindermann, Uchoa, Miller - Phys. Rev. B 86, 115415 (2012)
Abergel, Wallbank, Chen, Mucha-Kruczynski, Fal'ko - New J Phys 15, 123009 (2013)
San-Jose, Gutierrez, Sturla, Guinea - PRB 90, 115152 (2014)
Wallbank, Mucha-Kruczynski, Chen, Fal'ko - Ann. Phys. 527, 359 (2015)

Berry phase and Berry curvature for gapped secondary DPs:

$$\Phi = \int d^2 p \ \Omega$$

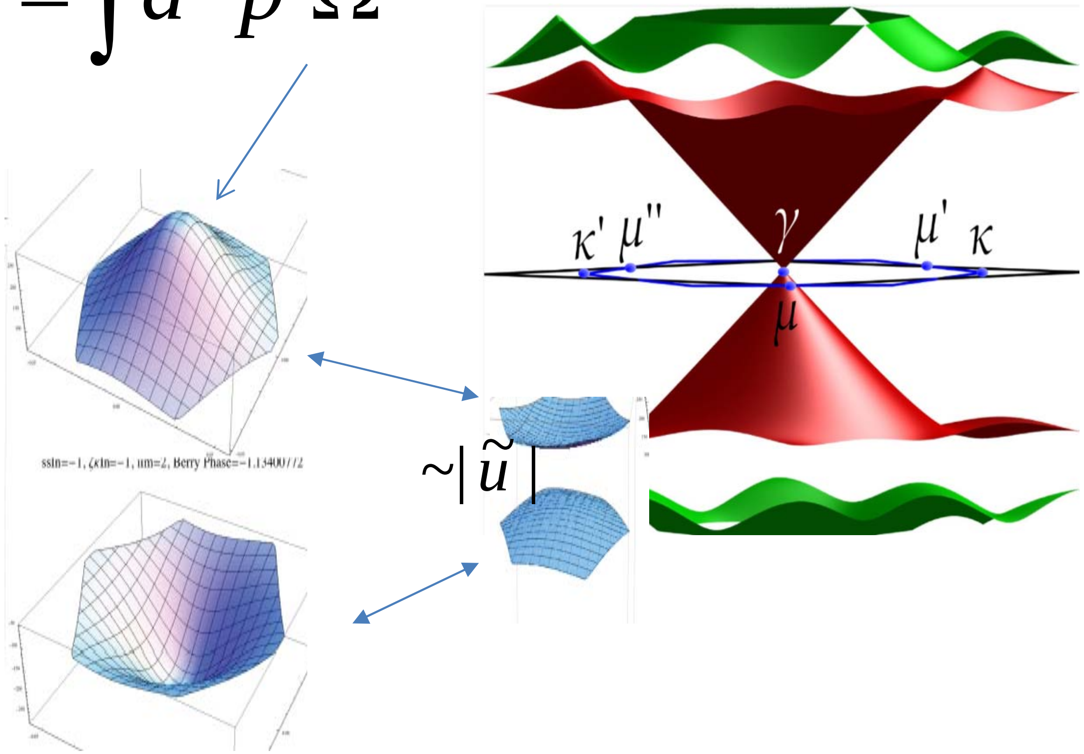

$$\Omega(\tilde{u} \to 0) \to \pm\pi\delta(\vec{p} - \vec{\kappa})$$

$$\Phi(\tilde{u} \to 0) \to \pm\pi$$

Wallbank, Mucha-Kruczynski, Chen, Fal'ko
Annalen der Physik, 527, 259 (2015)

Optical signature of moiré minibands

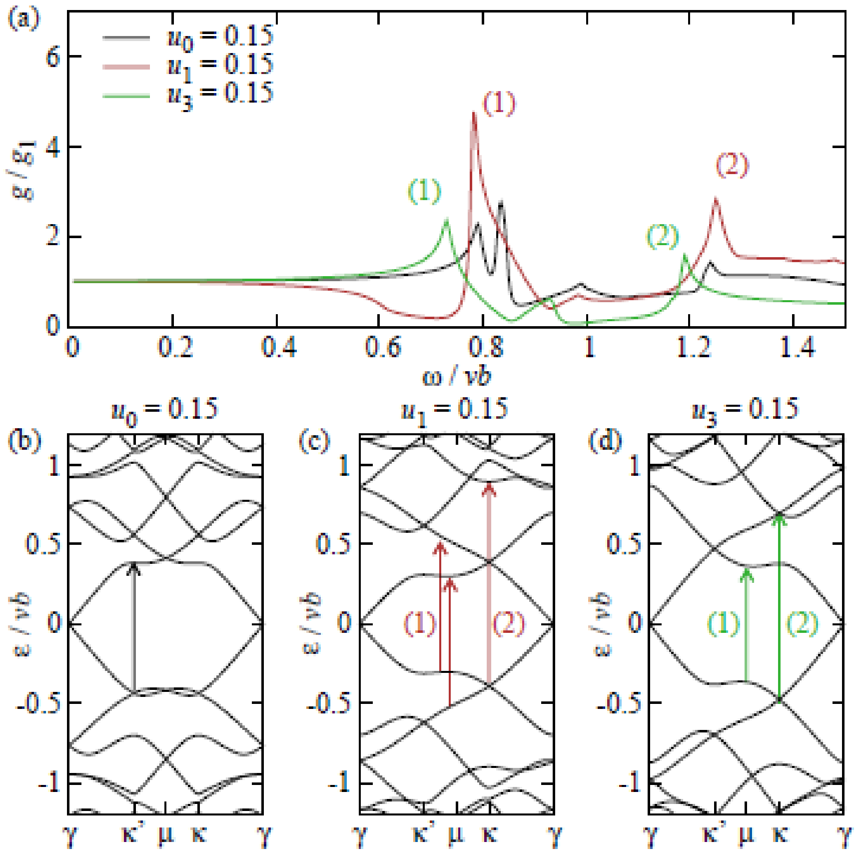

For better visibility should be enhanced by differentiation with respect to gate voltage/density

Abergel, Wallbank, Chen, Mucha-Kruczynski, Fal'ko
New J Phys 15, 123009 (2013)

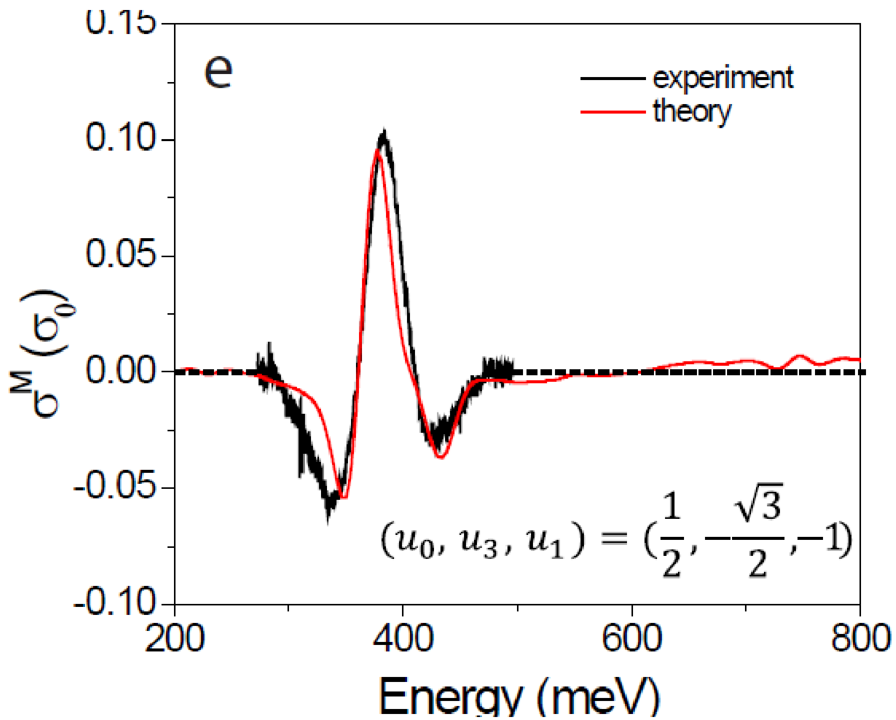

Shi, Jin, Yang, Ju, Horng, Lu, Bechtel, Martin, Fu, Wu, Watanabe, Taniguchi, Zhang, Bai, Wang, Zhang, Wang
Nature Physics 10, 743 (2014)

Manifestation of minibands in magneto-transport and capacitance spectroscopy

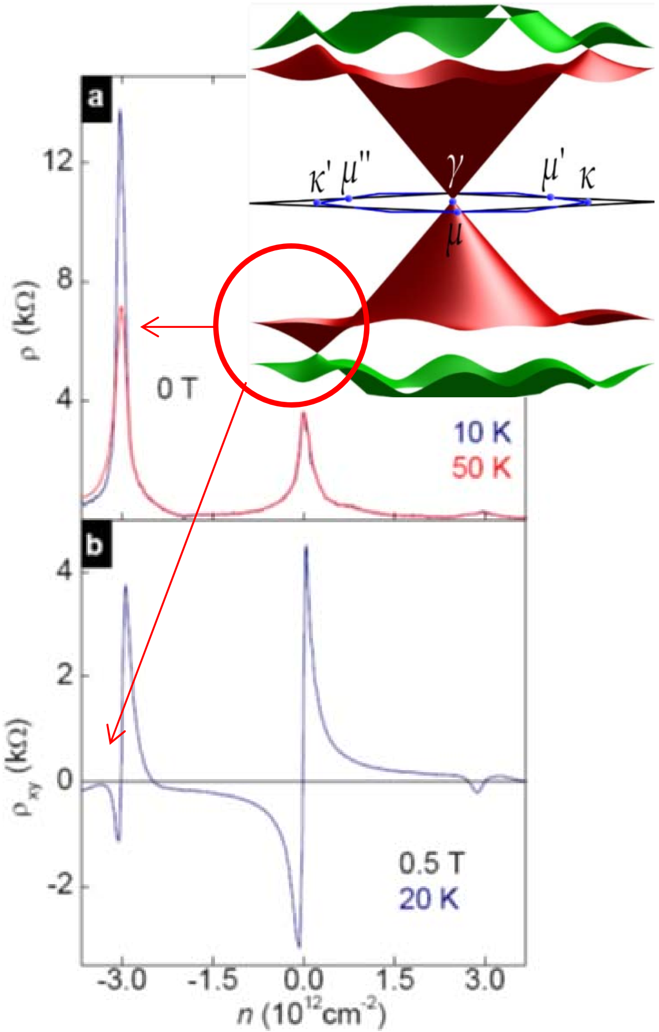

Ponomarenko, Gorbachev, Elias, Yu, Patel, Mayorov, Woods, Wallbank, Mucha-Kruczynski, Piot, Potemski, Grigorieva, Guinea, Novoselov, Fal'ko, Geim
Nature 497, 594 (2013)
Wallbank, Patel, Mucha-Kruczynski, Geim, Fal'ko
PRB 87, 245408 (2013)

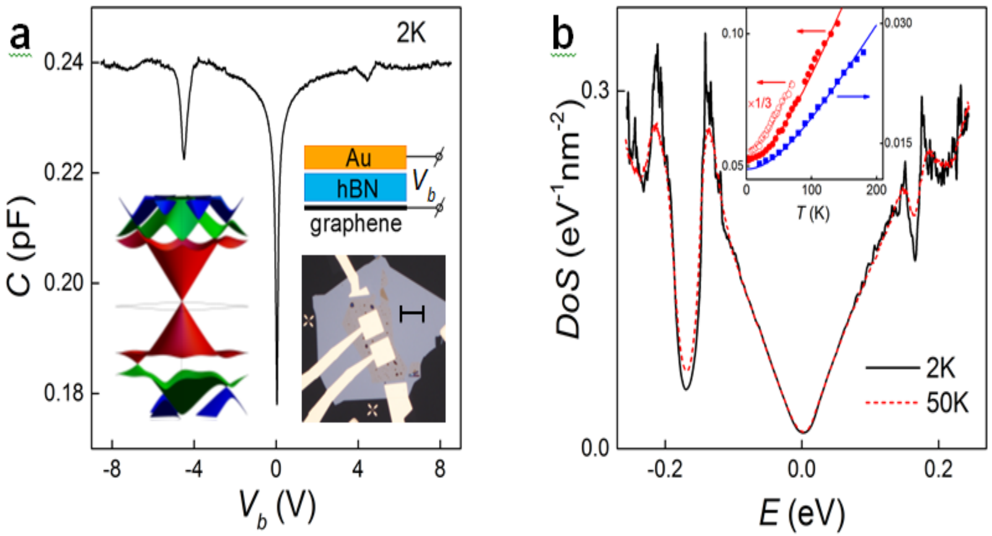

Yu, Gorbachev, Tu, Kretinin, Cao, Jalil, Withers, Ponomarenko, Chen, Piot, Potemski, Elias, Watanabe, Taniguchi, Grigorieva, Novoselov, Fal'ko, Geim, Mishchenko
Nature Physics 10, 525 (2014)

Transverse magnetic focusing of electrons in moiré minibands in almost aligned G/hBN

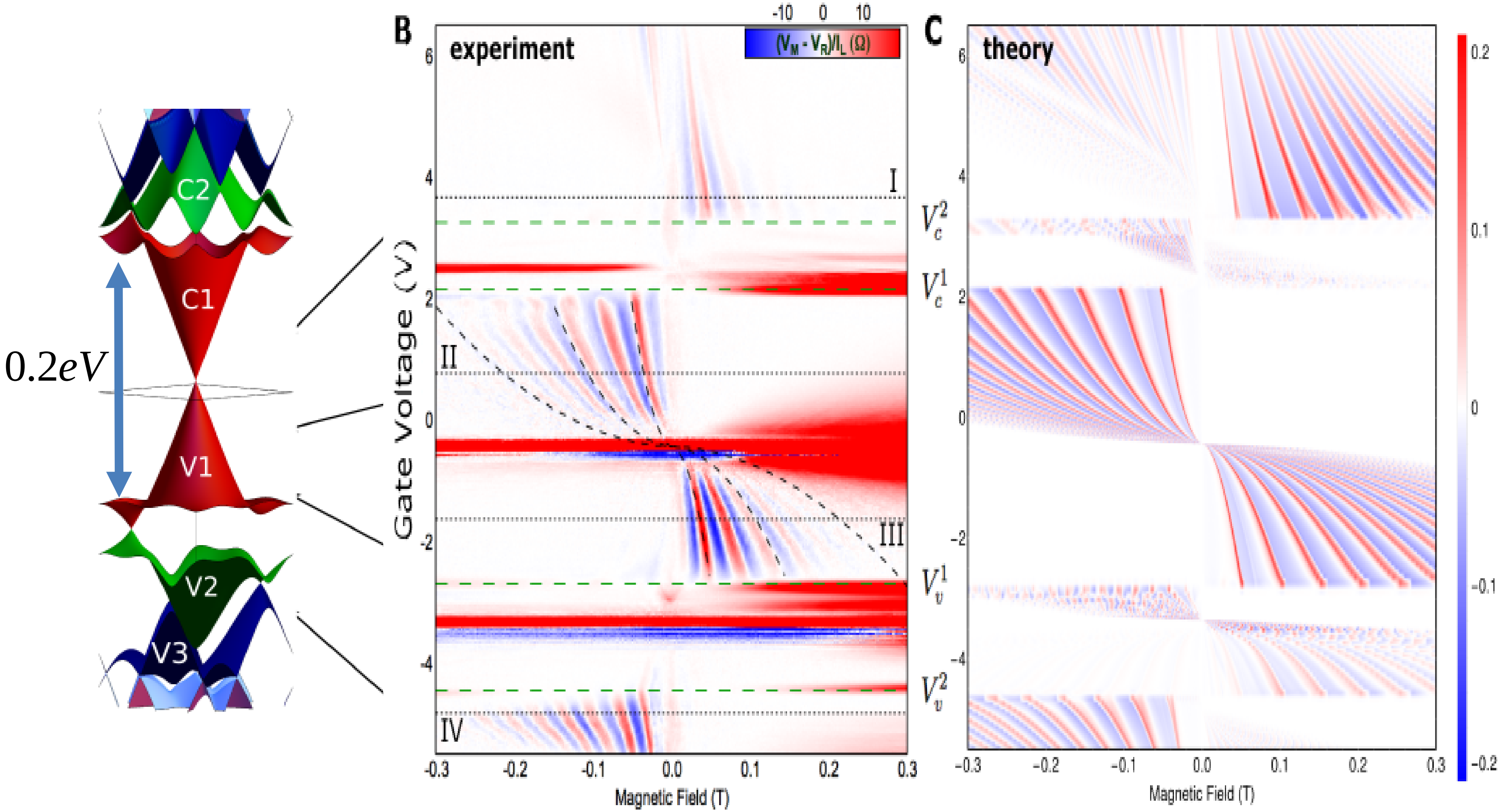

Lee, Wallbank, Gallagher, Watanabe, Taniguchi, Fal'ko, Goldhaber-Gordon - Science 353, 1526 (2016)

Landau levels of Dirac electrons in a magnetic field

$$H = v\left(\vec{p} - \tfrac{e}{c}\vec{A}\right)\cdot\vec{\sigma} \;\Rightarrow\; \varepsilon^{\pm} = \pm\sqrt{2n}\,\frac{v}{\lambda_B} \propto \sqrt{n\cdot B}$$

with *4*-fold degenerate Landau level

McClure - Phys. Rev. 104, 666 (1956)

the largest gaps in the LL spectrum

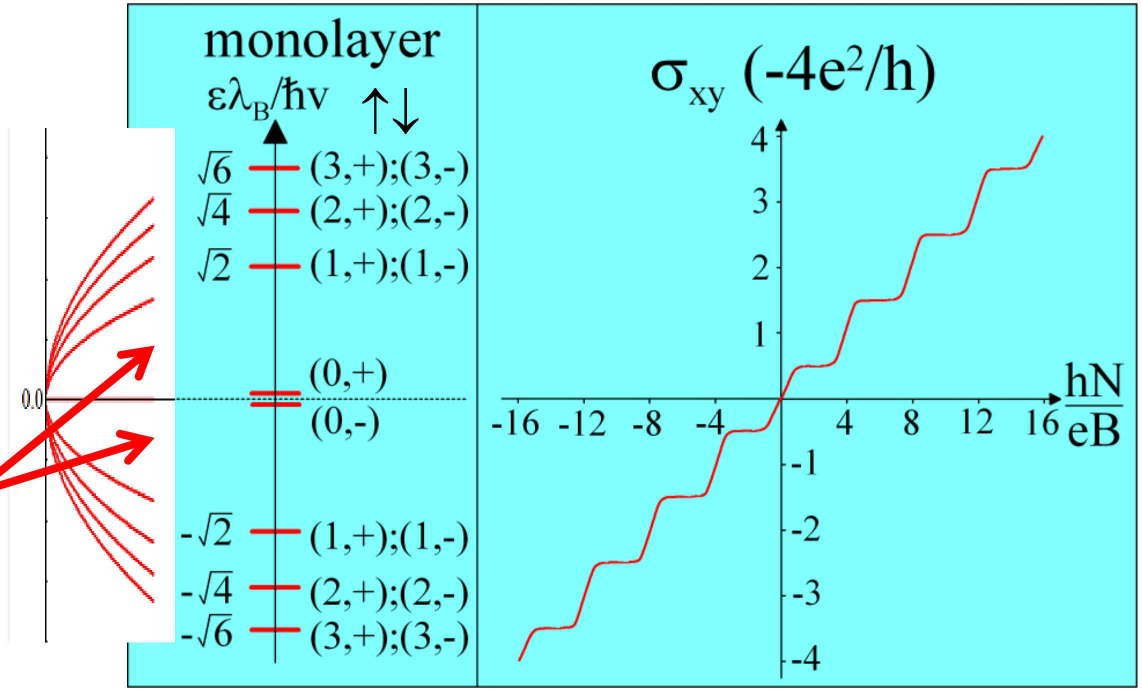

Should be the same for the secondary Dirac electrons at the edge of the 1st moiré miniband

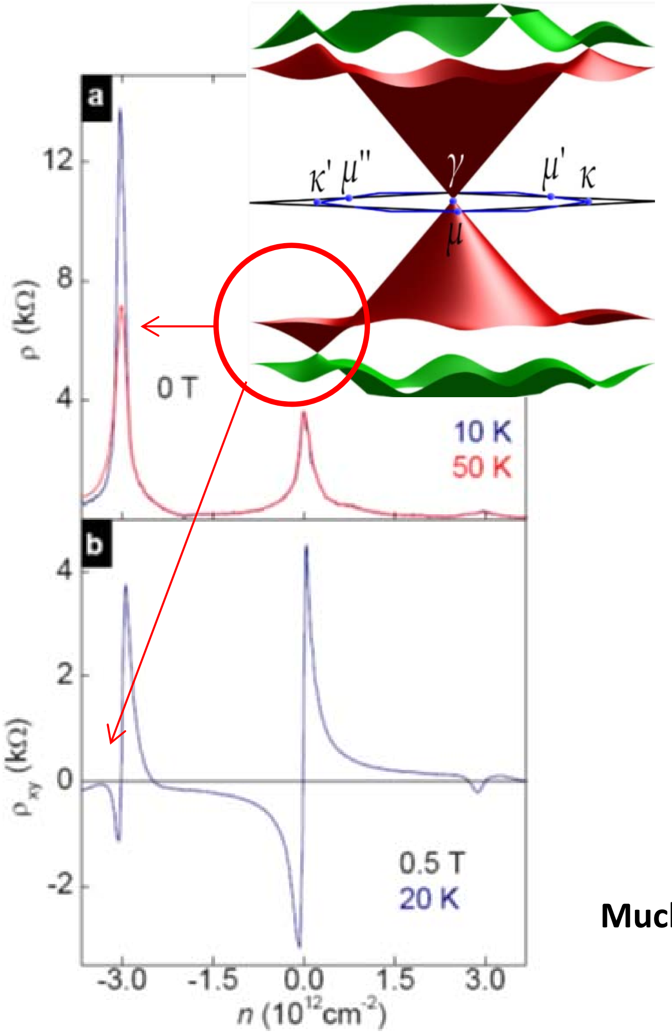

Magneto-transport in oriented graphene-BN heterostructures

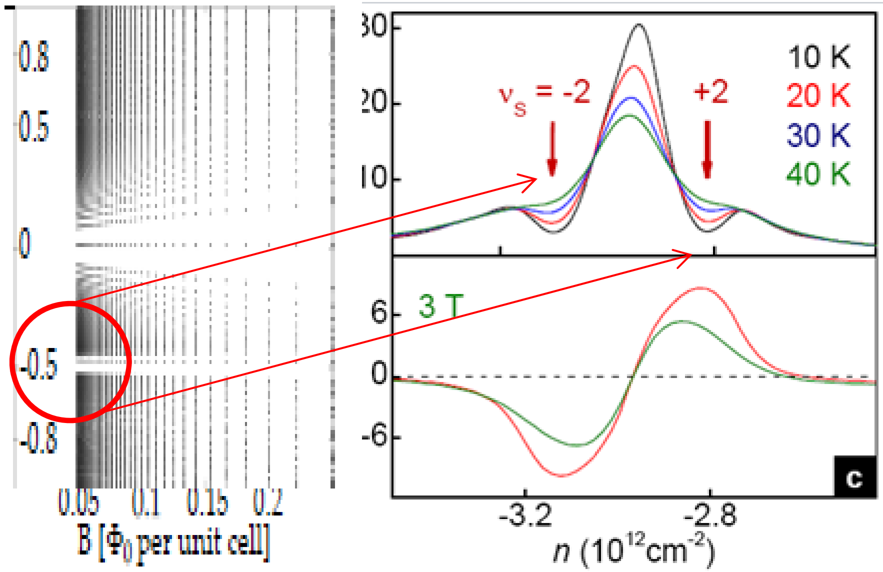

Wallbank, Patel, Mucha-Kruczynski, Geim, Fal'ko - PRB 87, 245408 (2013)
Ponomarenko, Gorbachev, Elias, Yu, Patel, Mayorov, Woods, Wallbank, Mucha-Kruczynski, Piot, Potemski, Grigorieva, Guinea, Novoselov, Fal'ko, Geim Nature 497, 594 (2013)

Magneto-capacitance

Yu, Gorbachev, Tu, Kretinin, Cao, Jalil, Withers, Ponomarenko, Chen, Piot, Potemski, Elias, Watanabe, Taniguchi, Grigorieva, Novoselov, Fal'ko, Geim, Mishchenko Nature Physics 10, 525 (2014)

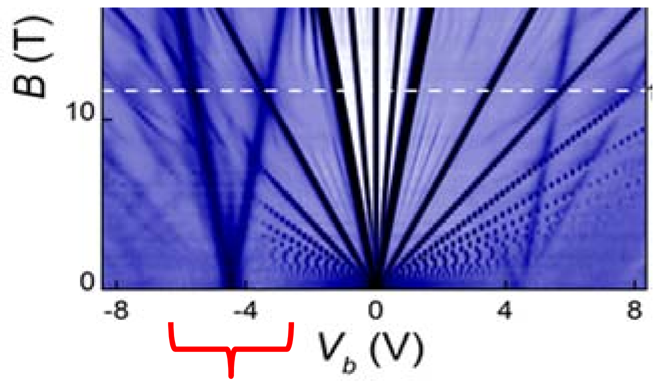

Quantum transport in graphene

L1 Disordered graphene (G)

L2 Ballistic electrons in graphene (G/hBN)

L3 Moiré superlattice effects in G/hBN heterostructures

tunnelling between almost aligned graphene flakes

moiré superlattice in van der Waals heterostructures

moiré minibands in G/hBN

Brown-Zak magnetic minibands in G/hBN

Brown, PR 133, A1038 (1964); Zak, PR 134, A1602 & A1607 (1964)

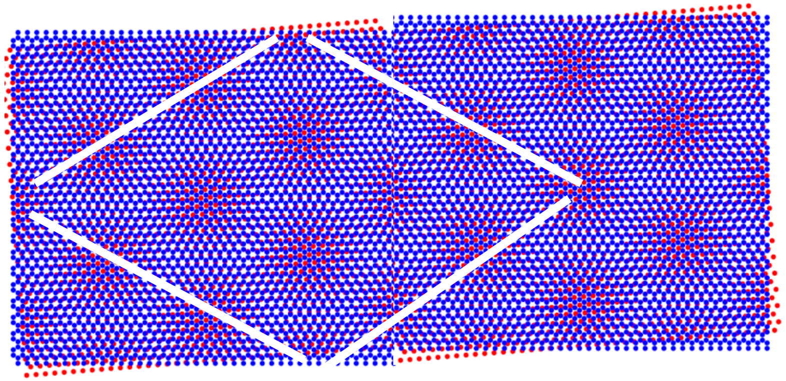

$$\phi \equiv BS = \frac{p}{q}\phi_0, \quad \phi_0 = \frac{h}{e}$$

Magnetic minibands at rational values of magnetic field flux per super-cell

'Magnetic lattice' with a q^2 times bigger effective supercell and q^2 times smaller mini Brillouin zone.

Each state in this mini Brillouin zone is q times degenerate.

Branded as fractal 'Hofstadter butterfly' spectrum.

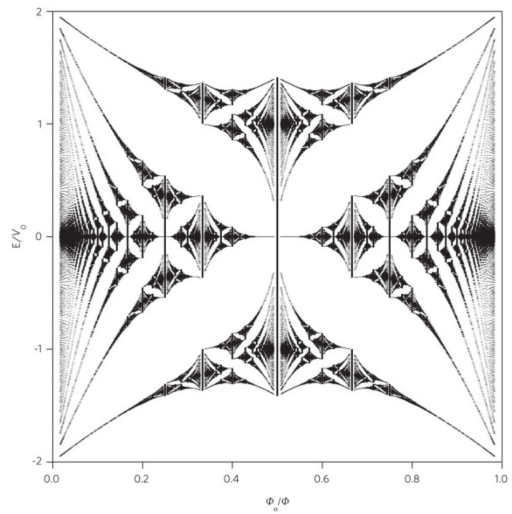

Example for the tight-binding model on a square lattice

Hofstadter PRB 14, 2239 (1976)

Brown - PR 133, A1038 (1964)
Zak - PR 134, A1602 & A1607 (1964)

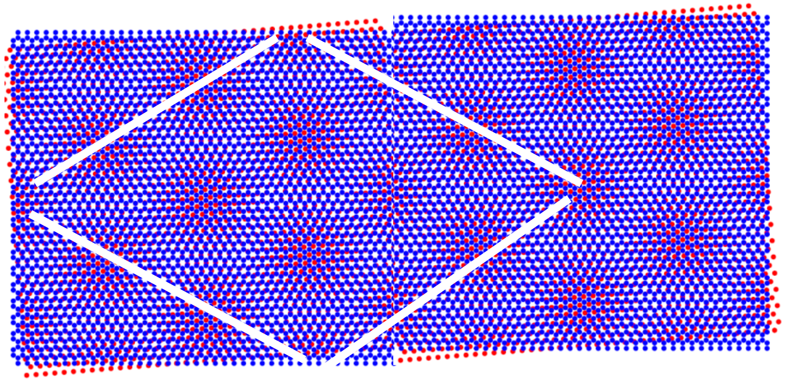

Zak-Brown magnetic minibands

$$\phi \equiv BS = \frac{p}{q}\phi_0$$

‘Magnetic lattice’ with a q^2 times bigger effective supercell and q^2 times smaller Brillouin mini-zone (over-folded).

Each state in this Brillouin mini-zone is q times degenerate.

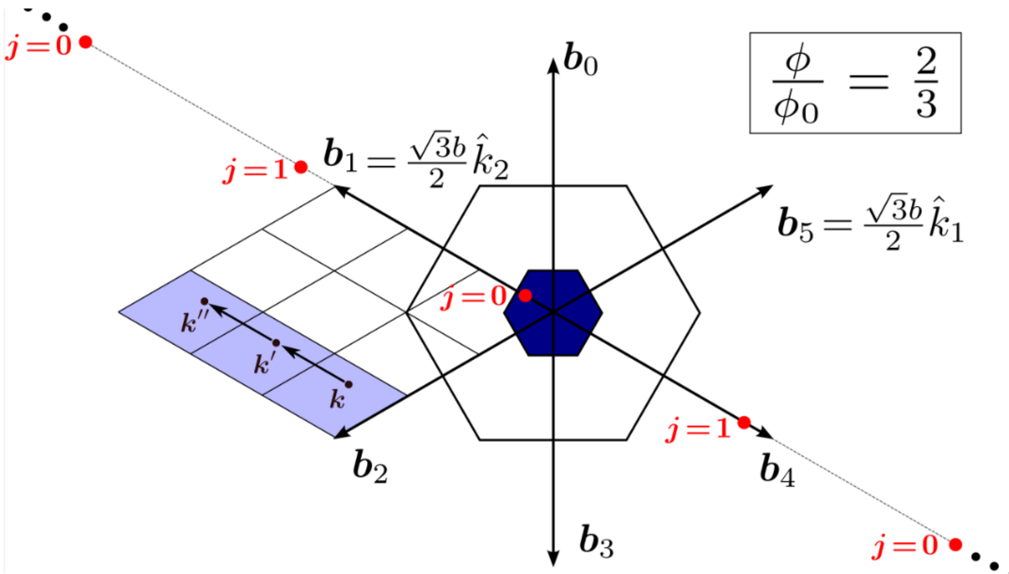

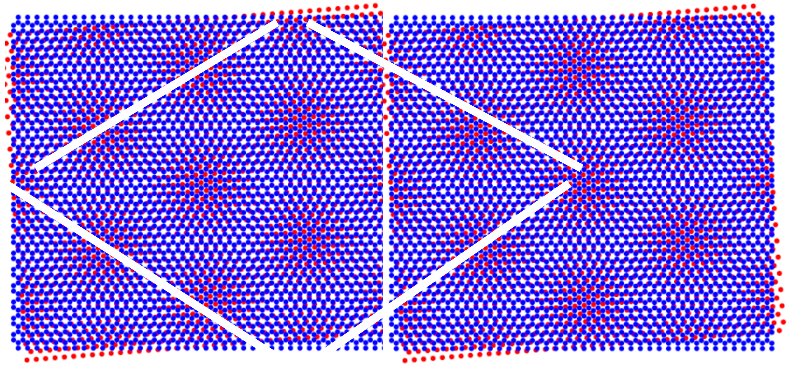

‘Magnetic lattice’ with a *9* times bigger effective supercell

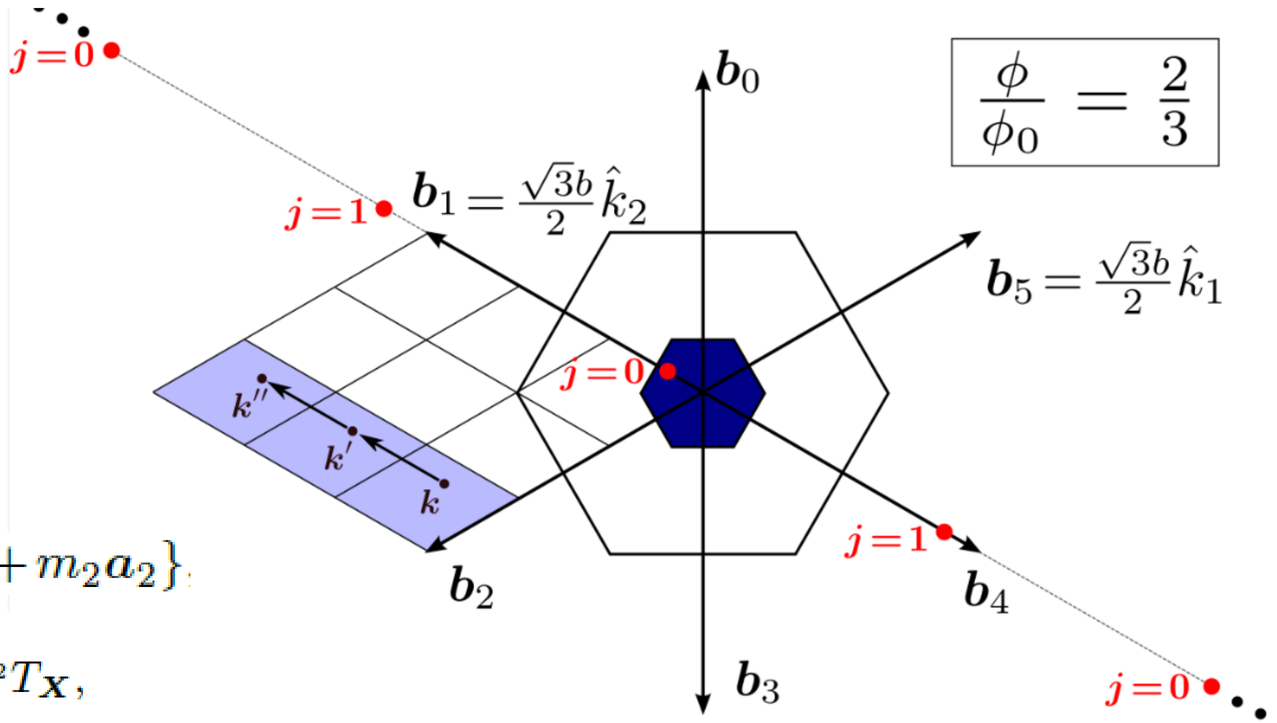

$$G_M = \{\Theta_{\boldsymbol{X}}, \boldsymbol{X} = m_1\boldsymbol{a}_1 + m_2\boldsymbol{a}_2\}$$

$$\Theta_{\boldsymbol{X}} \equiv e^{-ieBm_1 a\frac{\sqrt{3}}{2}x_2} T_{\boldsymbol{X}},$$

$$\Theta_{\boldsymbol{X}}\Theta_{\boldsymbol{X}'} = e^{-i2\pi\frac{p}{q}m_1' m_2}\Theta_{\boldsymbol{X}+\boldsymbol{X}'},$$

$$\Theta_{\boldsymbol{X}}\Theta_{\boldsymbol{X}'} = e^{-i2\pi\frac{p}{q}(m_1' m_2 - m_1 m_2')}\Theta_{\boldsymbol{X}'}\Theta_{\boldsymbol{X}}.$$

$$G_{qM} = \{\Theta_R, R = qm_1\vec{a}_1 + qm_2\vec{a}_2\} \subset G_M$$

For numerical diagonalization we used basis of LLs written in a hexagonal coordinate system

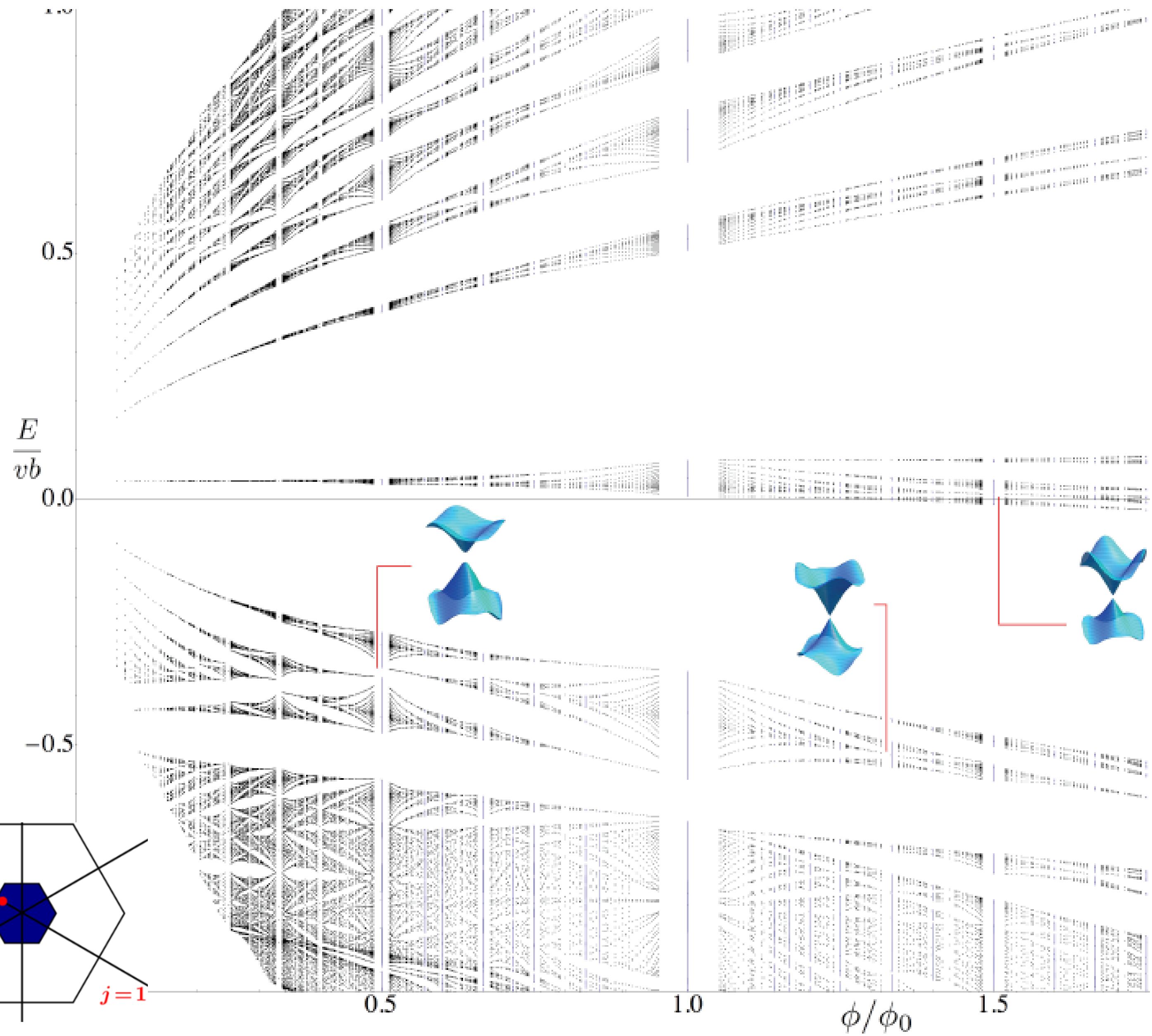

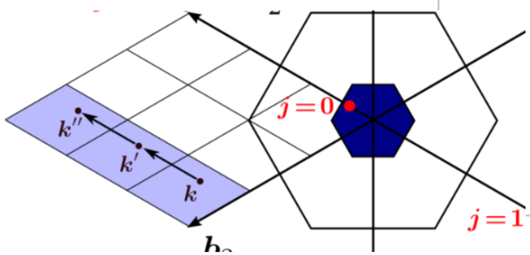

Chen, Wallbank, Patel, Mucha-Kruczynski, McCann, Fal'ko - PRB 89, 075401 (2014)

Magnetic minibands at $\phi = \frac{p}{q}\phi_0$ - gapped Dirac electrons

$$H_{Dirac} = v_{mDP}(\vec{k} - \tfrac{e}{c}\delta\vec{A})\cdot\vec{\sigma} + \tfrac{1}{2}\Delta\sigma_z$$

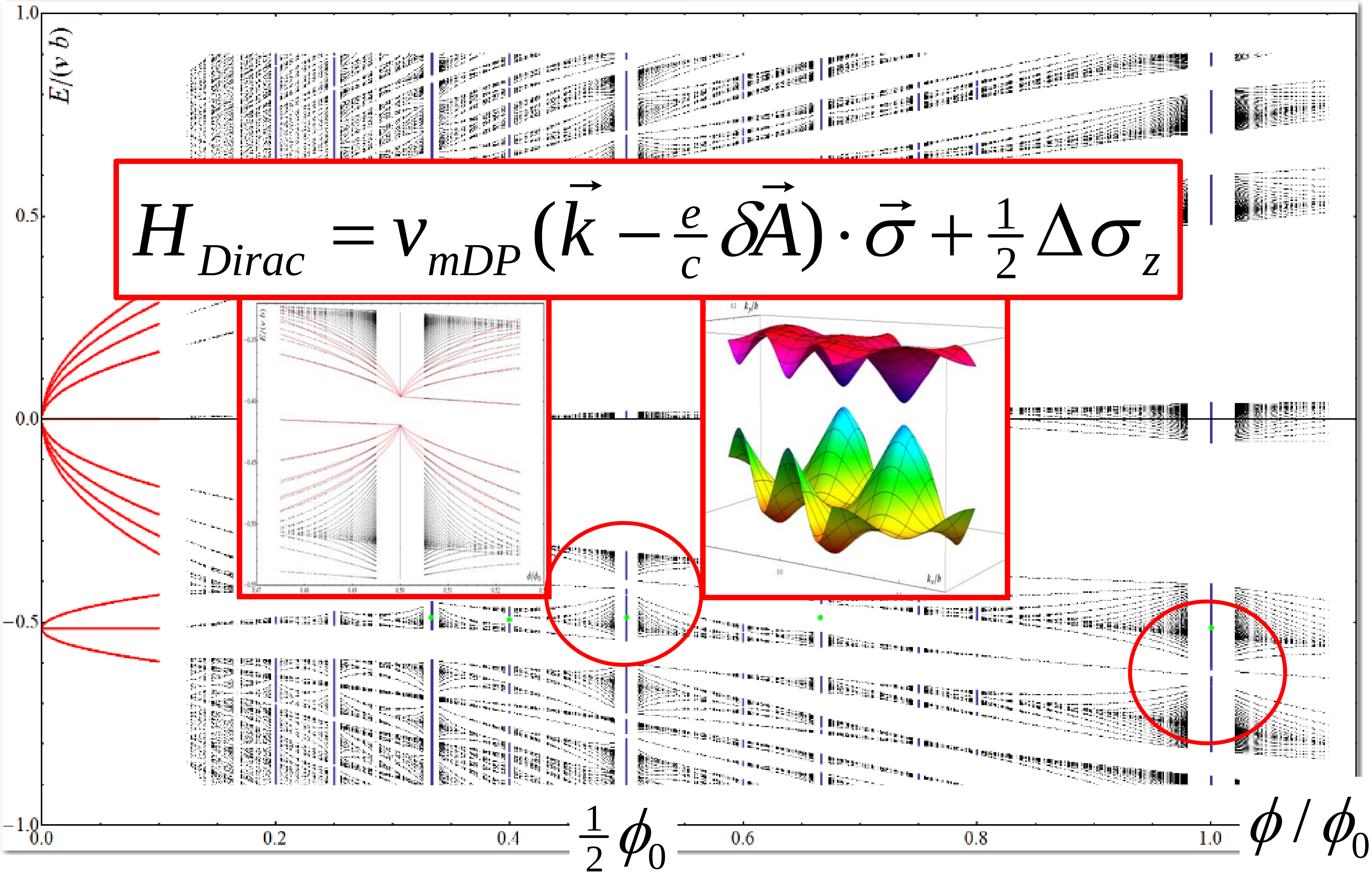

Chen, Wallbank, Patel, Mucha-Kruczynski, McCann, Fal'ko – PRB 89, 075401 (2014)

High-temperature Brown-Zak oscillations

Hierarchy of Brown-Zak minibands:

widest minibands at 1/N fractions; then at 2/(2N+1)

all others are much smaller.

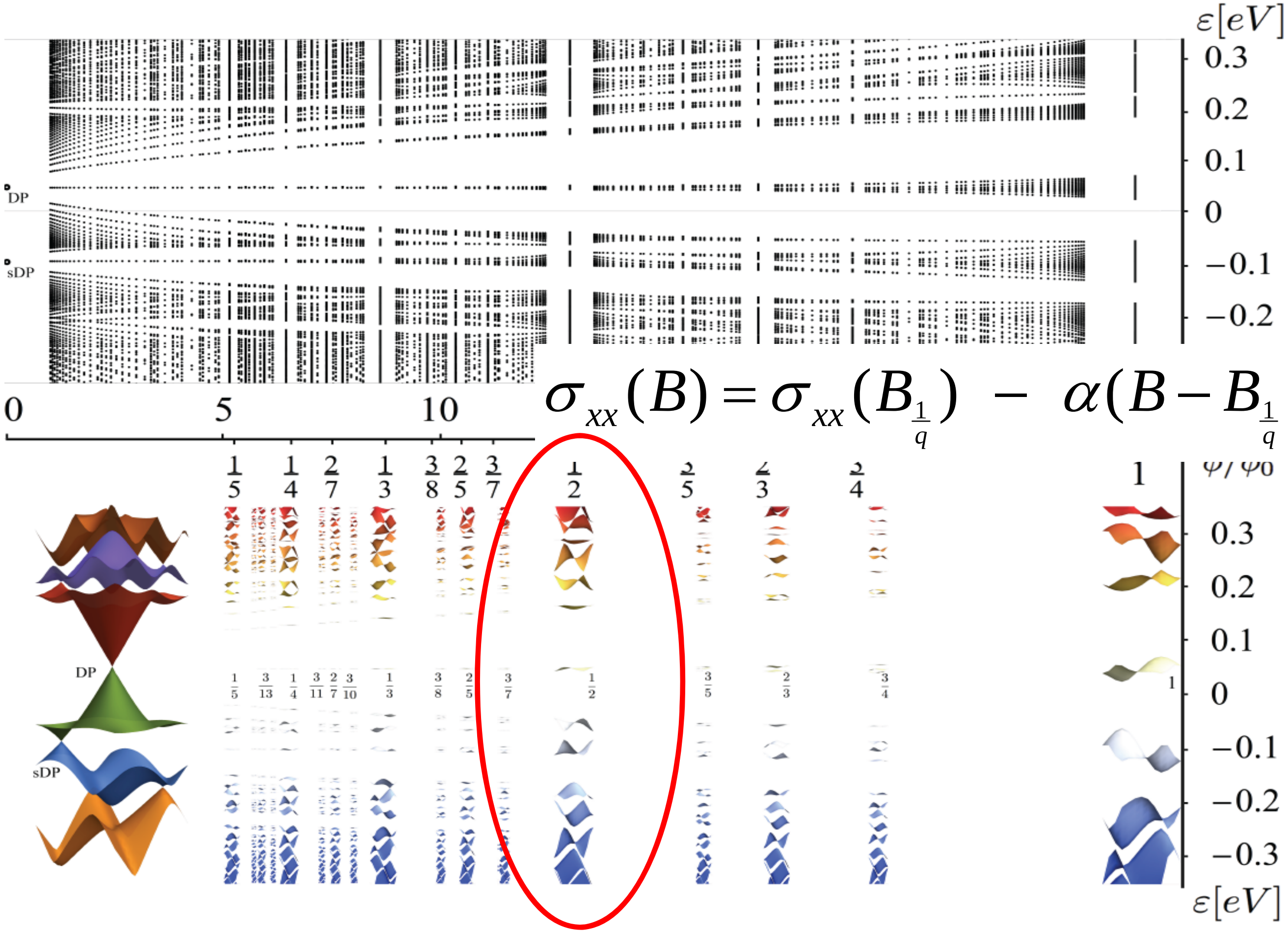

$$\sigma_{xx}(B) = \sigma_{xx}(B_{\frac{1}{q}}) - \alpha(B - B_{\frac{1}{q}})^2$$

$$\sigma_{xx} = \tfrac{1}{2} e^2 \gamma \tau v^2 \quad \underset{T >> \varepsilon_{band}, \hbar\omega_c}{\Longrightarrow} \quad \frac{2e^2}{h} \frac{\varepsilon_F \tau}{\hbar} \frac{\langle v^2 \rangle}{v_F^2}$$

High-temperature Brown-Zak oscillations

$$50 \div 200K > \varepsilon_{band}, \hbar\omega_c$$

● calculated

$$\sigma_{xx}(B_{p/q}) = \frac{2e^2}{h}\frac{\varepsilon_F \tau}{\hbar}\frac{\langle v^2 \rangle}{v_F^2}$$

scattering time determined by fitting one point, at $\Phi = 1/2\ \Phi_0$

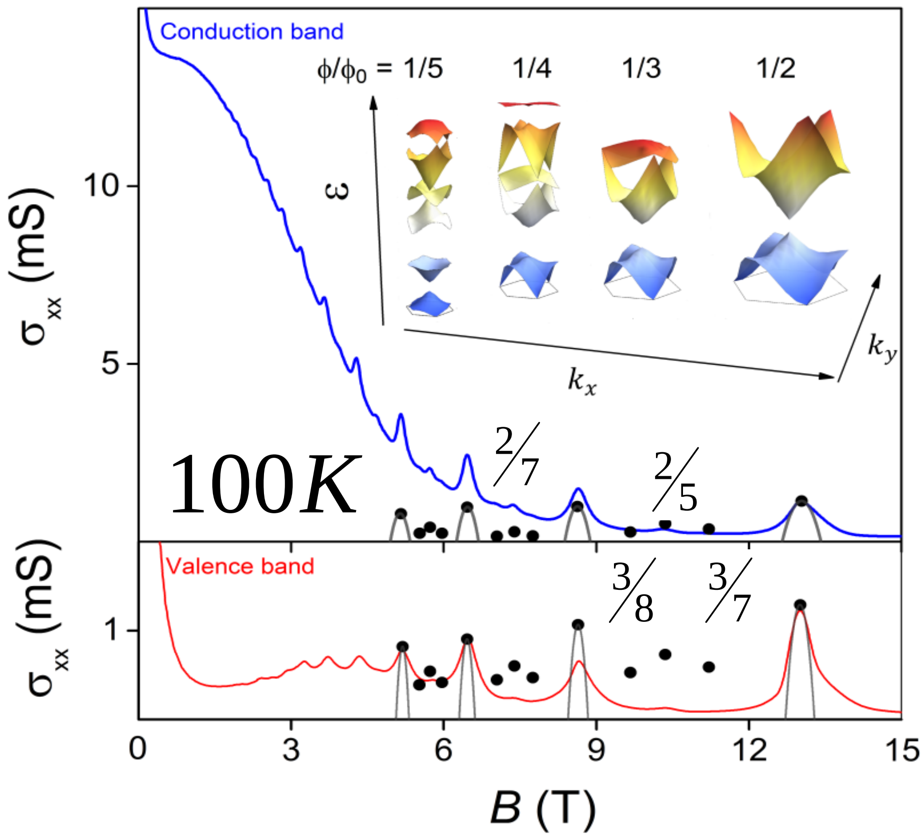

Krishna Kumar, Chen, Auton, Mishchenko, Bandurin, Morozov, Cao, Khestanova, Ben Shalom, Kretinin, Novoselov, Eaves, Grigorieva, Ponomarenko, Fal'ko, Geim - Science 357, 181 (2017)

Low-T magneto-transport and gaps between magnetic minibands

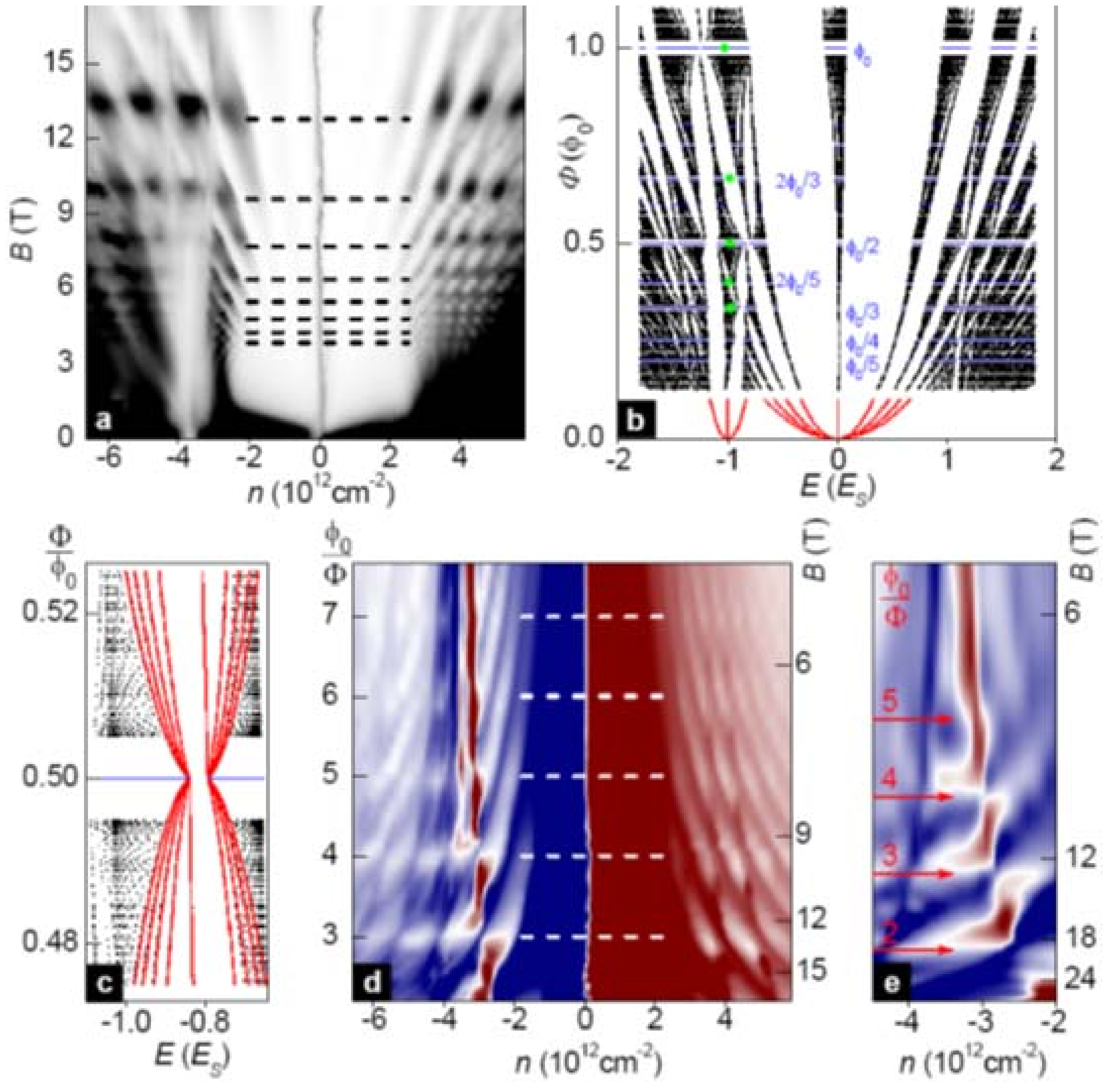

Ponomarenko, Gorbachev, Elias, Yu, Patel, Mayorov, Woods, Wallbank, Mucha-Kruczynski, Piot, Potemski, Grigorieva, Guinea, Novoselov, Fal'ko, Geim - Nature 497, 594 (2013)

Capacitance spectroscopy of gaps between magnetic minibands

Yu, Gorbachev, Tu, Kretinin, Cao, Jalil, Withers, Ponomarenko, Chen, Piot, Potemski, Elias, Watanabe, Taniguchi, Grigorieva, Novoselov, VF , Geim, Mishchenko - Nature Physics 10, 525 (2014)

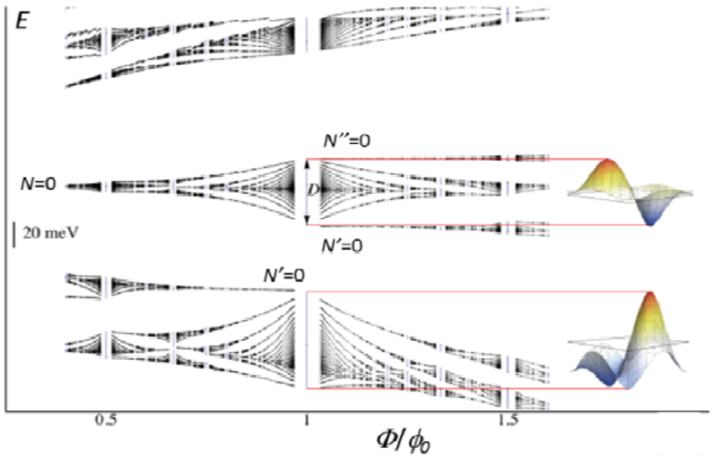

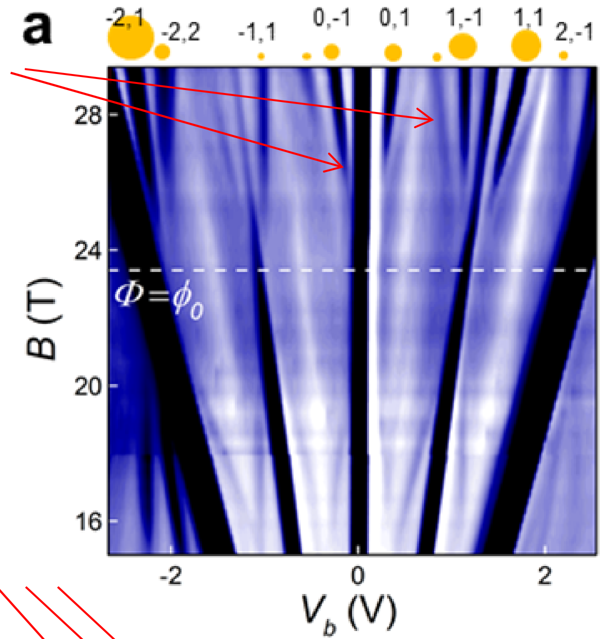

Ferromagnetic quantum Hall effect states in Landau levels of the third generation of Dirac electrons

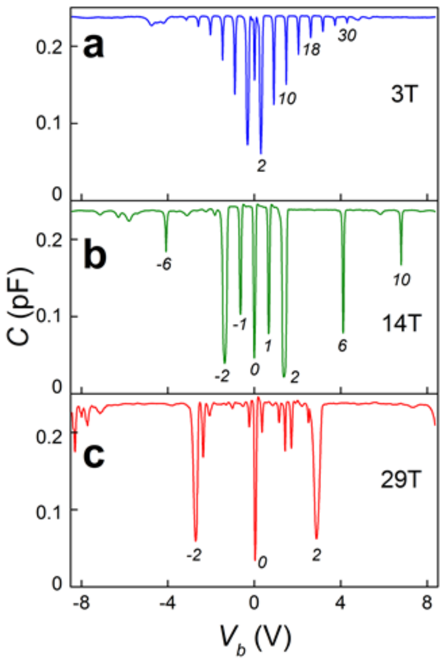

Gaps between Landau levels and incompressible ferromagnetic quantum Hall states of primary Dirac electrons

Gaps between Landau levels of secondary Dirac electrons

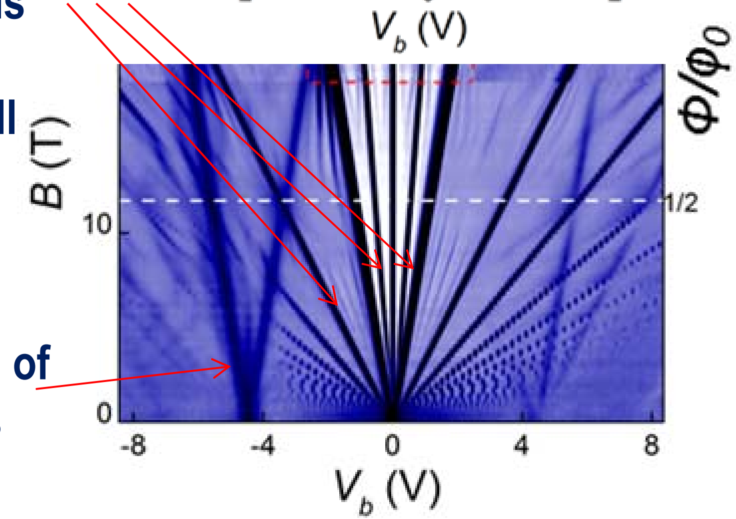

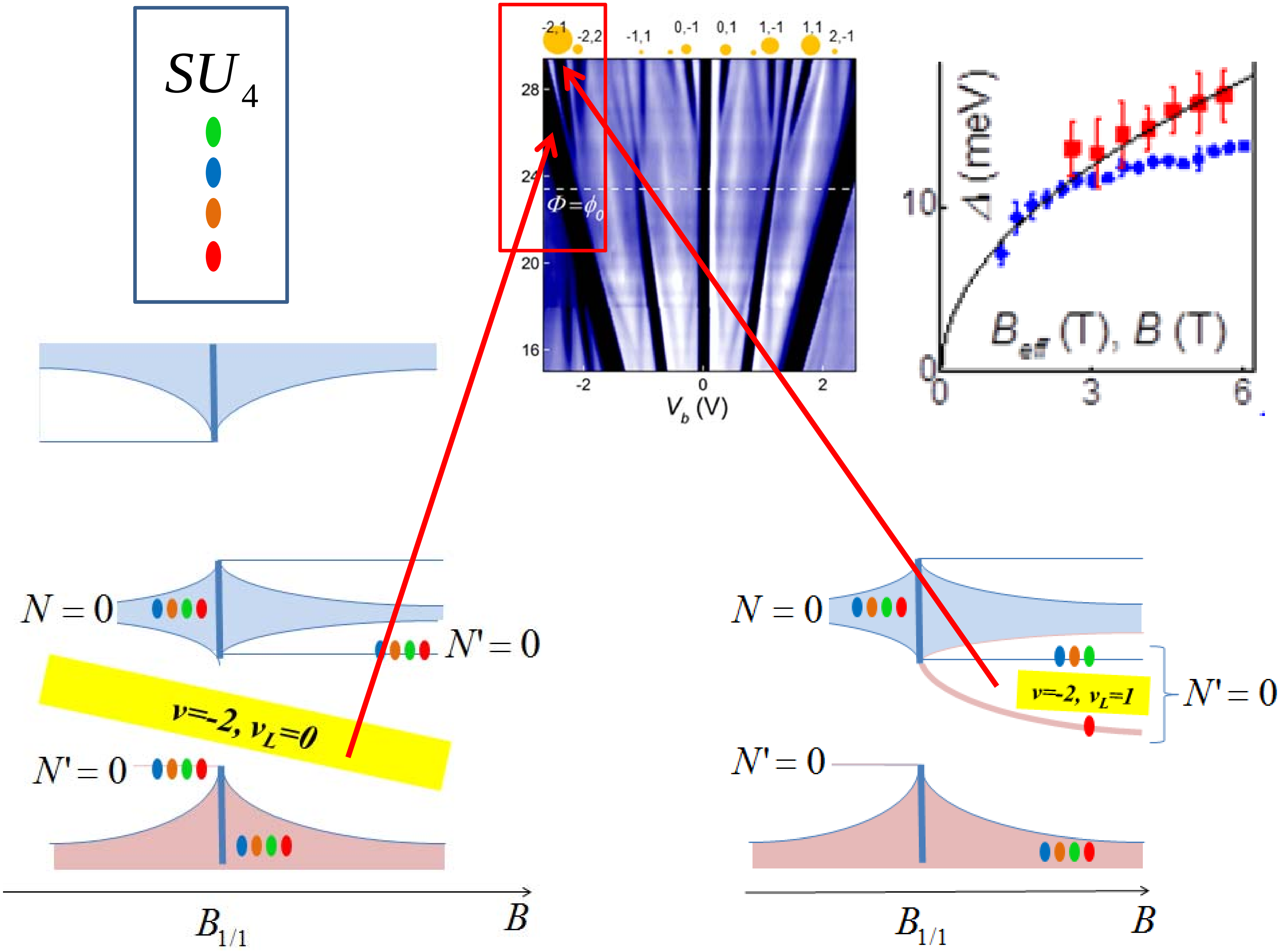

SU 4
-2,1
-2,2
-1,1
0,-1
0,1
1,-1
1,1
2,-1
28
24
20
16
Φ=φ0
-2
0
2
V_b (V)
Δ (meV)
10
0
B_eff (T), B (T)
0
3
6
N = 0
N' = 0
ν=-2, ν_L=0
N' = 0
B_1/1
B
N = 0
ν=-2, ν_L=1
N' = 0
N' = 0
B_1/1
B

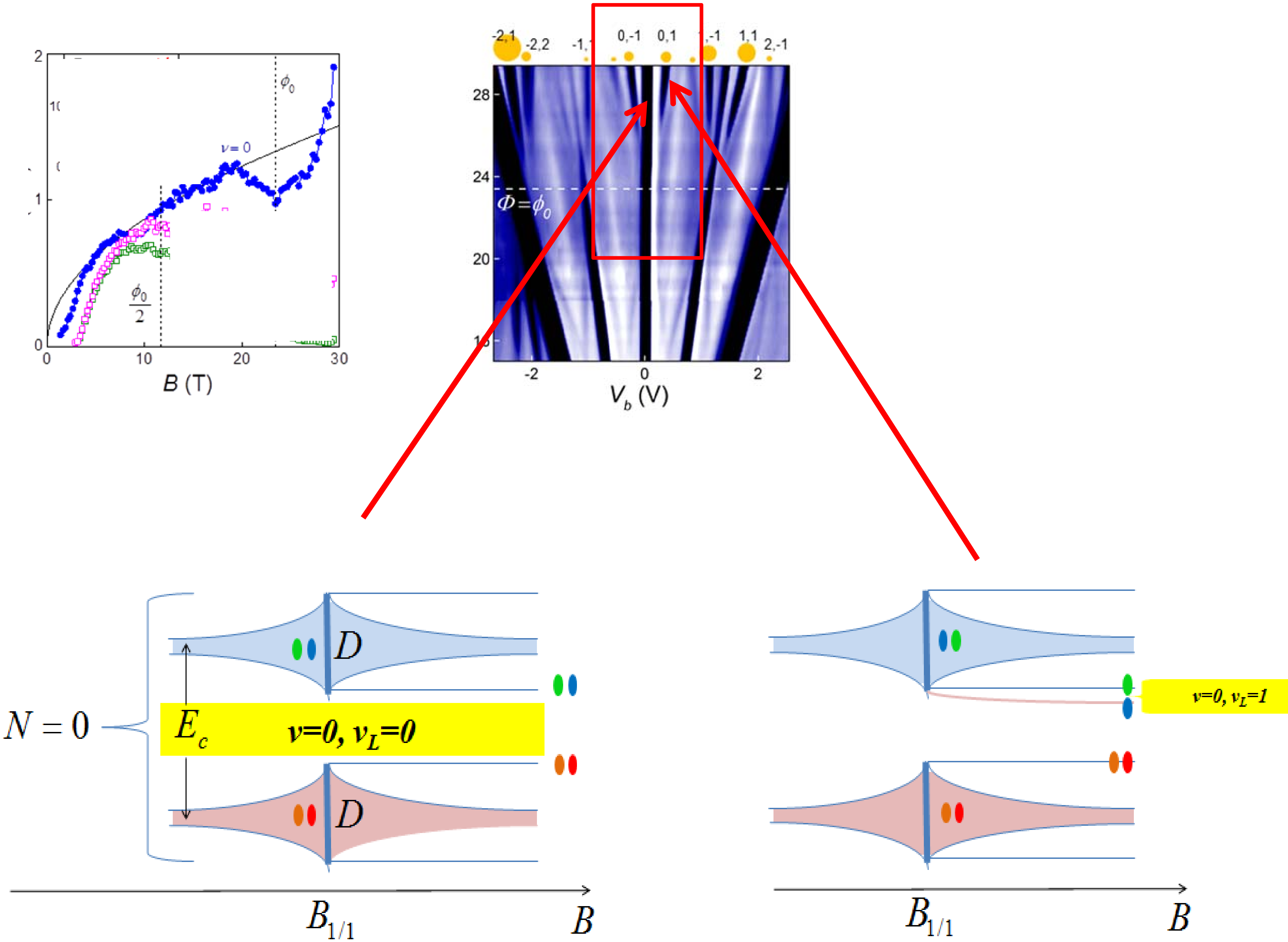

ν = 0
ϕ_0
$\frac{\phi_0}{2}$
B (T)
-2,1
-2,2
0,-1
0,1
1,1
2,-1
$\Phi=\phi_0$
V_b (V)
D
D
E_c
ν=0, ν_L=0
N = 0
ν=0, ν_L=1
$B_{1/1}$
B
$B_{1/1}$
B

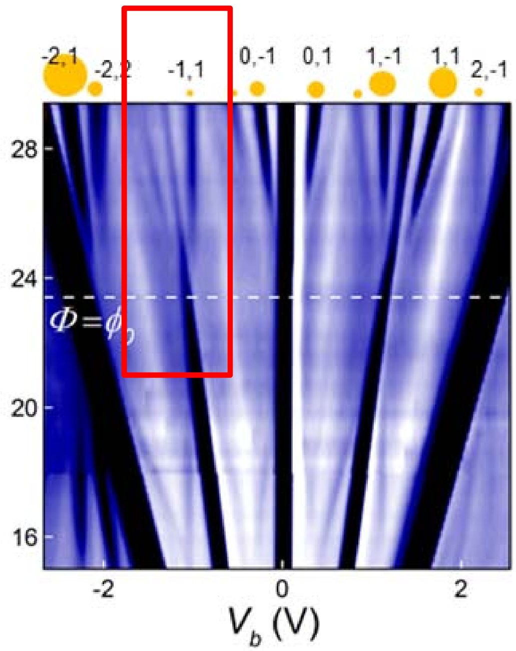

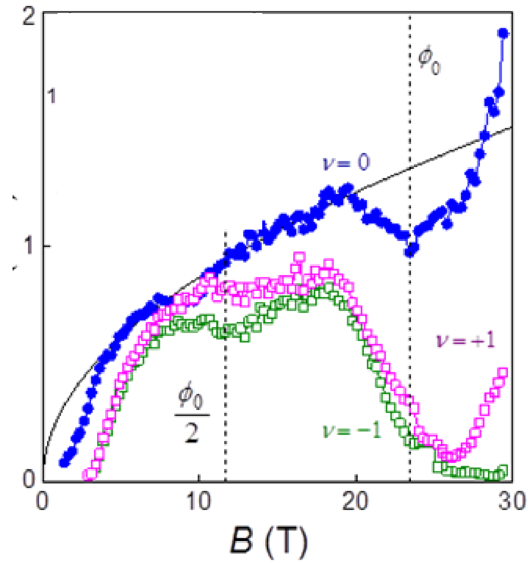

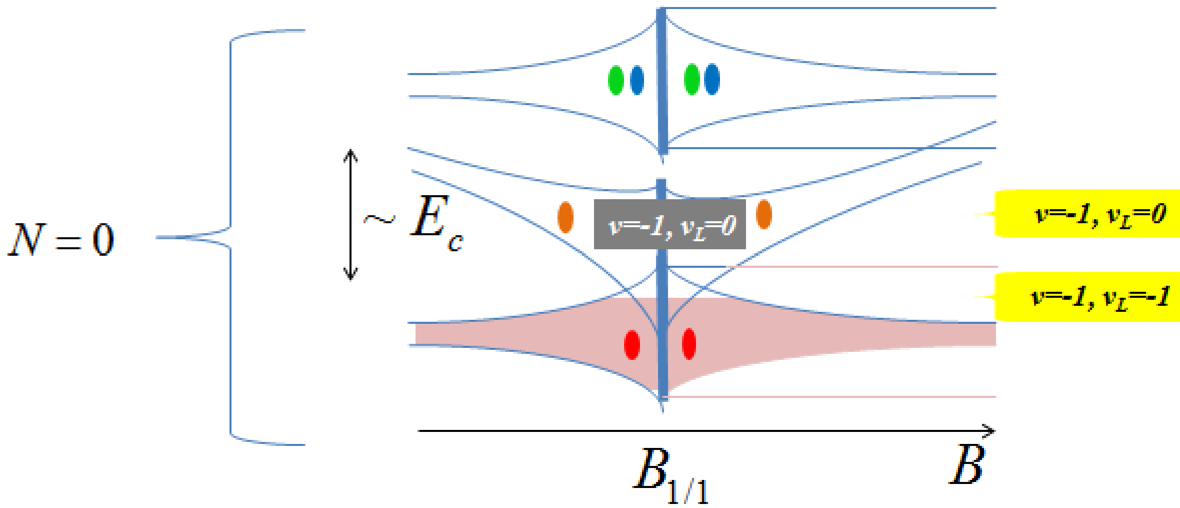

Reverse Stoner transition

Extreme quantum physics in moiré superlattice:

- ✓ moiré minibands for electrons
- ✓ Zak-Brown magnetic minibands / 'Hofstadter butterfly'

Xi Chen (NGI)
John Wallbank (NGI)
Marcin Mucha-Kruczynski (Bath)
David Abergel (Nordita)

Andre Geim (NGI)
Marek Potemski (CNRS-Grenoble)
David Goldhaber-Gordon (Stanford)
Takashi Taniguchi (NIMS)

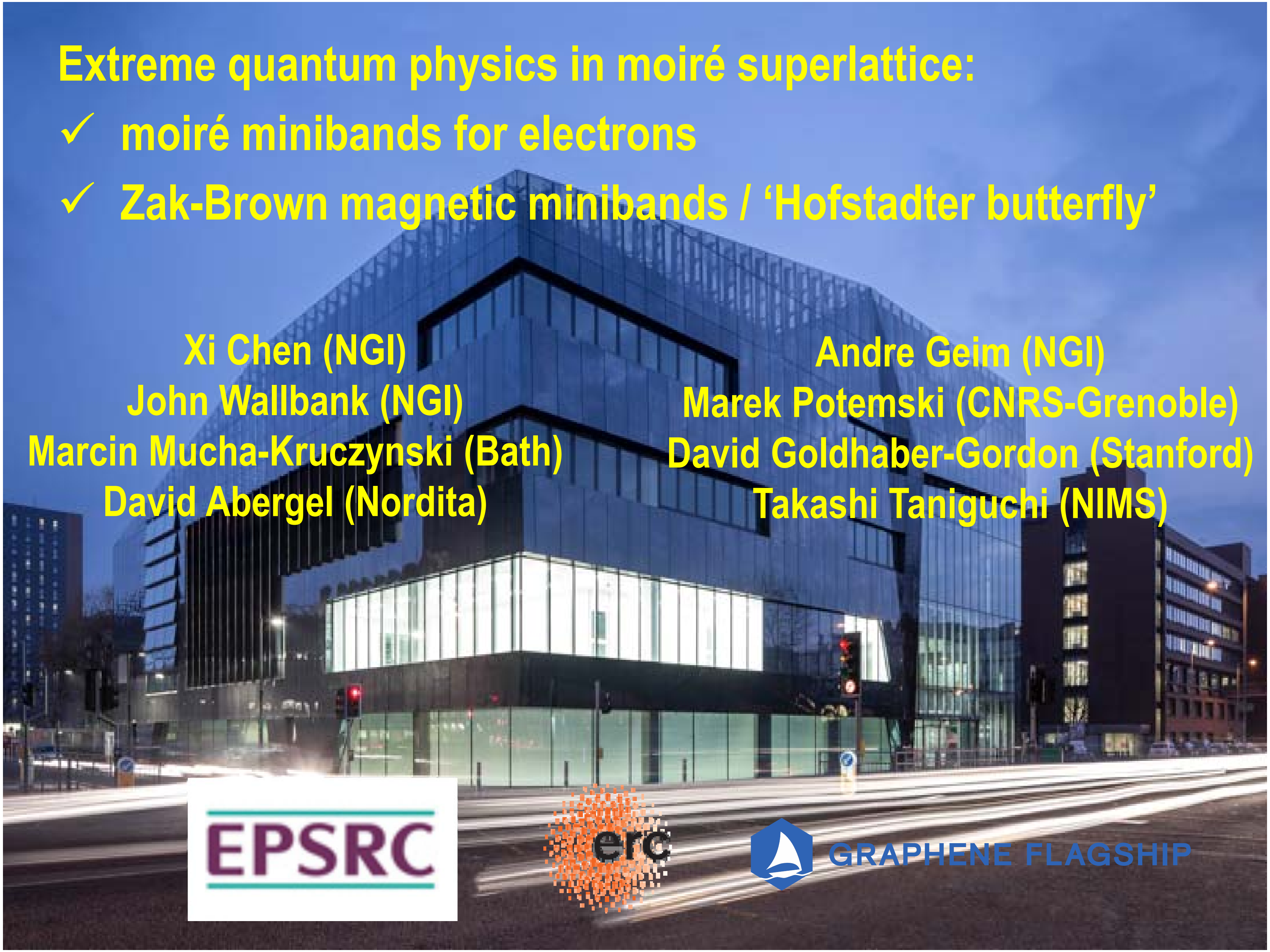

honeycomb graphene on weakly-coupled insulating honeycomb hBN

↓

one of the atoms in the unit cell affects graphene orbitals stronger than the other.

↓

one sublattice defines a simple hexagonal lattice.

inversion non-symmetric

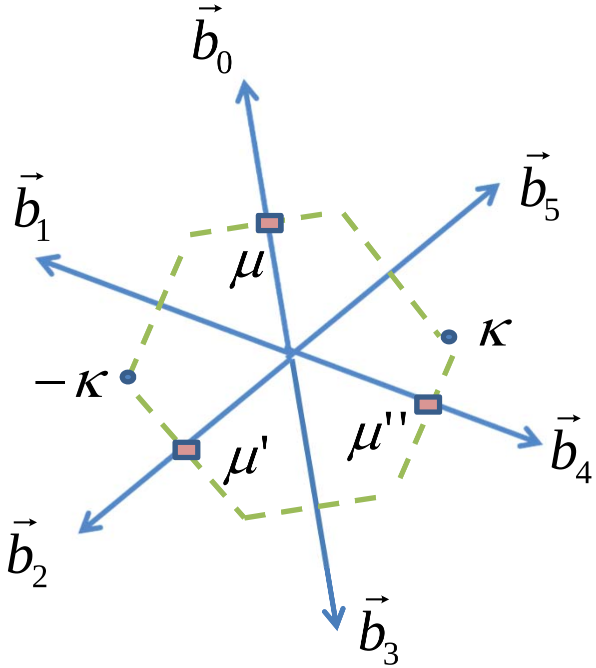

inversion symmetric with a small asymmetric addition

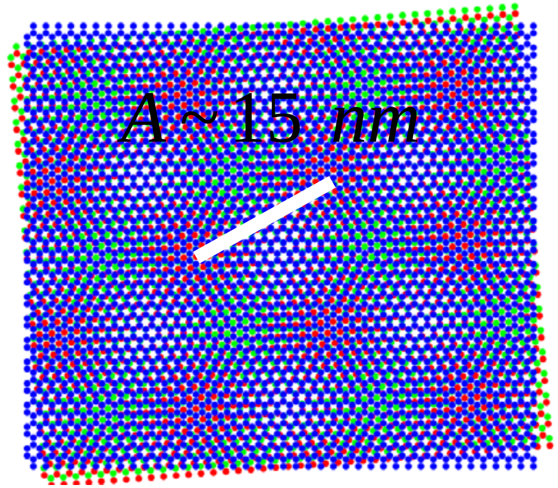

$$A \approx \frac{a}{\sqrt{\delta^2 + \theta^2}}$$

misalignment

lattice mismatch 1.8% for G/hBN

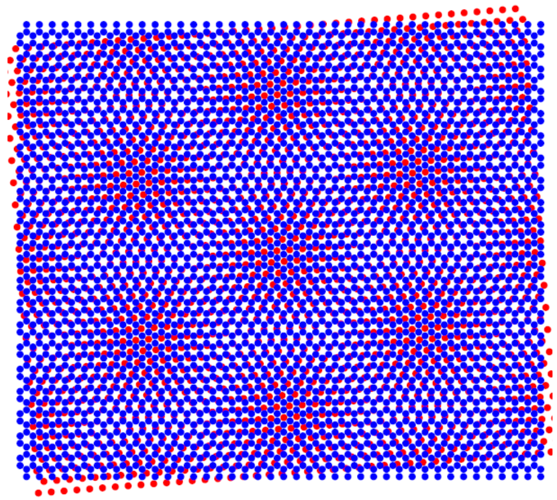

$$\hat{H} = vp\cdot\boldsymbol{\sigma} + u_0 vbf_1(r) + u_3 vbf_2(r)\sigma_3\tau_3 + u_1 v\left[\boldsymbol{l}_z \times \nabla f_2(r)\right]\cdot\boldsymbol{\sigma}\tau_3$$

3 mini-DPs at the edge of 1st miniband no e-h symmetry

single mini-DP at the edge of 1st miniband e-h symmetry

single mini-DP at the edge of 1st miniband in both c/v bands

generic: single mini-DP at the edge of 1st miniband no e-h symmetry

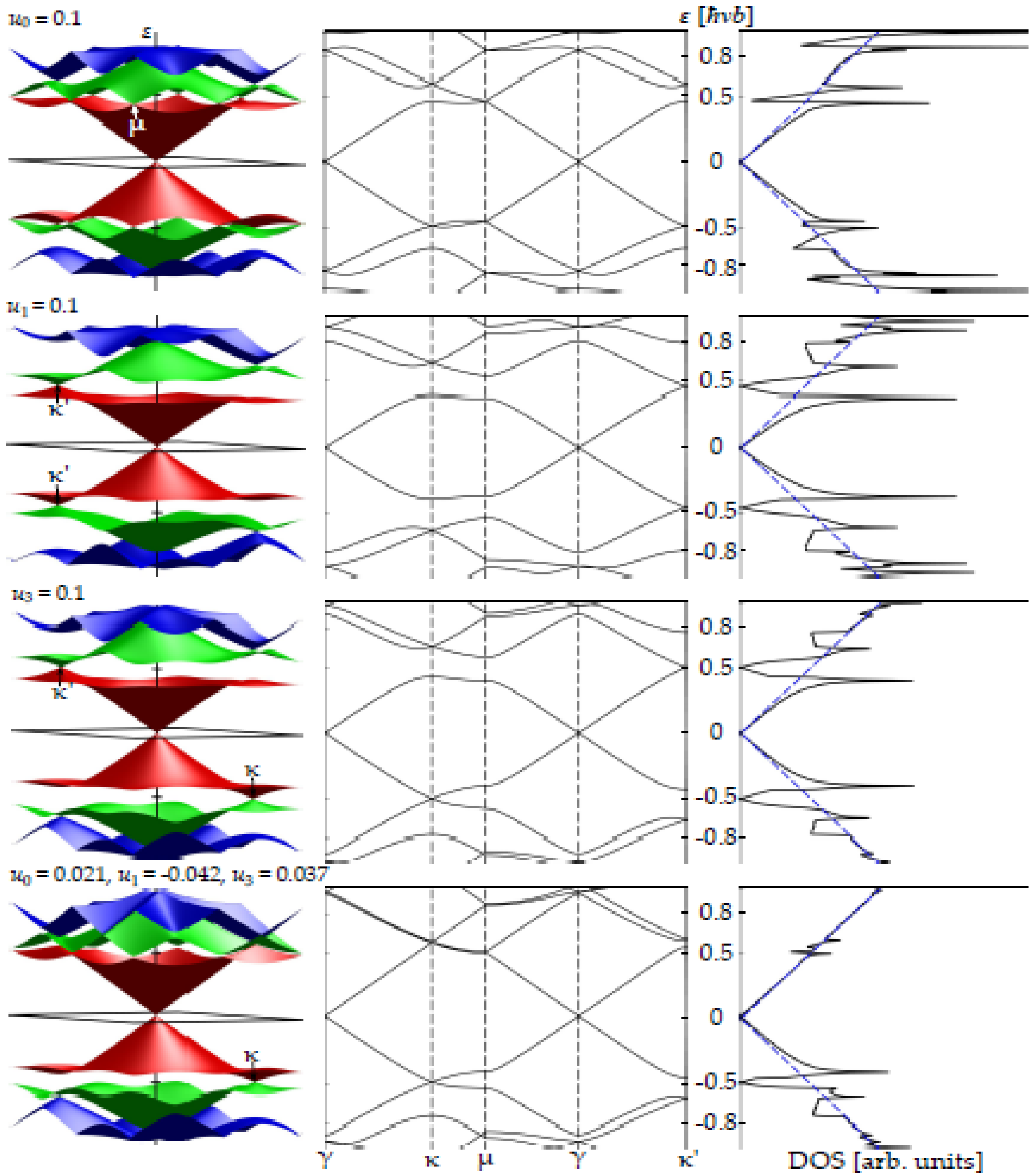

Wallbank, Patel, Mucha-Kruczynski, Geim, VF - PRB 87, 245408 (2013)